CHAPTER 4 INTERPRETATION

In the center of Eburru Crater, the sequences of the resistivity layers at the points A–17.5, A–20 and A–22.5 differ from those of all other soundings in the Eburru Geothermal Prospect. Those at the points A–17.5, A–20 and A–22.5 are that the lower resistivity layer overlies the thick higher resistivity layer. On the contrary, at the other points, the thick low resistivity layer is under thin high resistivity surface layer. The possible reasons why the thick high resistivity layer underlies the thin low resistivity layer only at the points A–17.5, A–20 and A–22.5 are as follows:

1. very compact intrusive rocks exist under the points A–17.5, A–20 and A–22.5,
2. air-filled space, for instance being caused by many cracks, under the concerned area is predominant,
3. rocks under the concerned area have been locally altered by hydrothermal activities and formed very compact rocks,
4. pore spaces of the rocks under the concerned area do not contain enough water because of high temperature or some other reason or the combination of some or all of them.

Because the gravity map of the area (U.N.D.P., 1972) does not show any significant gravity anomaly in Eburru Crater, we cannot assume any significant density change of rocks in Eburru Crater. Therefore the reason (1) is very unlikely in Eburru Crater. It is impossible without any further geological information to infer which is the most likely cause of the thick high resistivity layer underlying the thin lower resistivity layer only in Eburru Crater. This resistivity sequence might be very local because the results of dipole mapping survey by Group Seven for U.N.D.P. (1972) do not show any significant resistivity change at and around Eburru Crater.

In the east of Eburru Crater and along the lines C and D, the underlying thick low resistivity layer is very thick. It is considered that its thickness is at least 300 m and in some place, like at the point C–95, it is as thick as or over 900 m. It is infered that the underlying resistive layer under the above mentioned low resistivity layer might be compact basement rocks. The basement-like resistive layer is detected only at a few points. At the other sounding points, because the apparent resistivity curves do not show any sign of the existence of underlying resistive layer even by the maximum current electrode separation, half of which is 500 m at the edge of the survey lines and 1,500 m at the middle of the survey lines, the top of the basement-like resistive layer must be deeper than 500 m from the surface.

The resistivity of the thick low resistivity layer varies between 10 Ωm and 30 Ωm. The cause of its resistivity variation may be change of the porosity of the rocks or change of the salinity of the pore water. Without further knowledge of the underground geology, the nature of all the geoelectrical layering and changes cannot be defined. The resistivity interface might be an interface of a rock formation, an underground water table or significant change of temperature.

In Eburru Station Area, the similar resistivity interface of the overlying resistive layer and the underlying low resistivity layer is measured at the depth between 10 m and 110 m. At the points M–95, M–100, M–110, M–115, O–114, P–95, Q–99, Q–119 and Q–124, the underlying low resistivity layer is devided into an upper higher resistivity layer with resistivity of 30 Ωm and 70 Ωm and an underlying lower resistivity layer with it of between 6 Ωm and 25 Ωm. At the other sounding points, the underlying low resistivity layer may be divided into the same two layers. The upper higher resistivity layer may not be thick enough or the resistivity contrast may not be large enough to cause significant indication on the Schlumberger resistivity sounding curve.

In Eburru Station Area, unlike Eburru Crater Area, we could not see any high resistive basement layer on the sounding curves. Therefore, the high resistive basement must be deeper than 700 meter if there is any. Because of the altitude change around 2,000 m at Eburru Station Area and around 2,600 m at Eburru Crater Area, water table is nearer to the surface at Eburru Station Area than at Eburru Crater Area. It might have caused the very thick low resistivity layer in Eburru Station Area.

The only Schlumberger sounding in Eburru Station Area which shows the underlying thick resistive layer being covered by the low resistivity layer is at the point P–115. At the point P–115 the resistive layer with resistivity of 120 Ωm is covered by the low resistivity layer with resistivity of 20 Ωm. Because this sounding is the only sounding showing the underlying resistive layer, the resistive layer might be falsely shown due to electromagnetic coupling. However, there also exist a possibility of the underlying resistive layer at the point P–115 being an intrusive rock or an upheaval of basement rocks.

In Cedar West Area, the general feature of the resistivity layering is similar to those of Eburru Crater Area and Eburru Station Area. The thick low resistivity layer is covered by the resistive layer. Generally at the center of the valley the resistivity of the underlying thick low resistivity layer is lower than that at the side of the valley.

Along the H line, the resistivity of the underlying thick low resistivity layer varies very little. At the I line, the sounding curves of the three points are clearly devided into two types, the one at the point I–113 at the center of the valley and the other at the points I–103 and the I–123 at the sides of the valley. At the former one the low resistivity layer with the resistivity of 15 Ωm is covered by a series of the thin high resistivity layers with the resistivity of between 40 Ωm and 450 Ωm. At the latter the relatively high resistivity layer with resistivity of between 110 Ωm and 140 Ωm is covered by a series of the higher resistivity layers with resistivity between 280 Ωm and 1000 Ωm. Near the point I–113 there is a large alteration zone where condensed water is collected, and altitude of the point P–113 is several tens of meter lower than those of the Point I–103 and I–123. It is infered that the lower elevation of the area may provide a pass of hot underground water where the alterations are and the resistivity is lower than that of the area in higher elevation. This evidence supports the genetic model of Eburru Geothermal Area in Fig. 5.

The Table IV–1 shows the statistics of apparent resistivities at AB/2 = 500 m. On the table the mean value of the resistivity along the line E is much higher than those along the lines A, C and D. The line E is at the top of the fringe of the Eburru Crater and the other three lines are in and the east side of the crater. Therefore the difference of average elevation in those two groups of the lines is 50 m to 100 m. Thus the genetic model of Eburru Geothermal Area (Fig. 5) can explain the resistivity change by only the distance between the surface of the ground and the underground water table and also the position of heat source which is presumed under Eburru Crater.

REFERENCES

JICA Geothermal Mission, 1980, Interim report on geothermal exploration project in the Rift Valley.

JICA Geothermal Mission, 1981, Interim Report (II) on geothermal exploration project in the Rift Valley.

Keller, G.V. and Frischknecht, F.C., 1966, Electrical methods in geophysical prospecting, Pergamon Press, London.

Koefoed, O., 1979, Geosounding principles, 1. Elsevier, Amsterdam.

Orellana, E. and Mooney, H.M., 1966, Master tables and curves for vertical electrical sounding over layered structures, Interciencia, Madrid.

Parkhomenko, E.L., 1969, Electrical properties of rocks, Translated and edited by G.V. Keller, Plenum Press, New York.

U.N.D.P., 1972, Technical review meeting chairman's report, by James Healy.

Fig IV – 4 (I)

VES Curve and Computer Model, Point E108

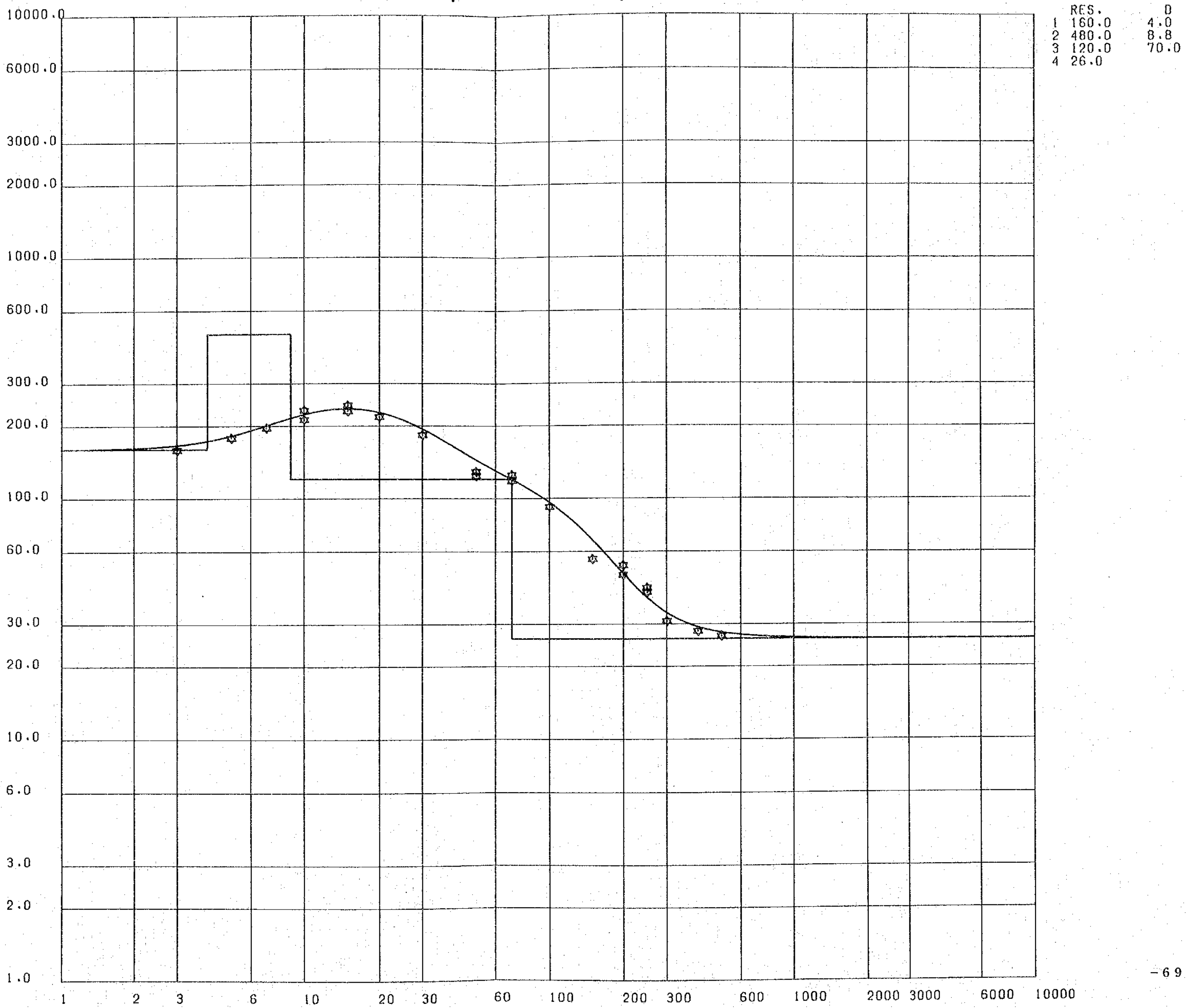

Fig IV-4 (2)

VES Curve and Computer Model, Point E113

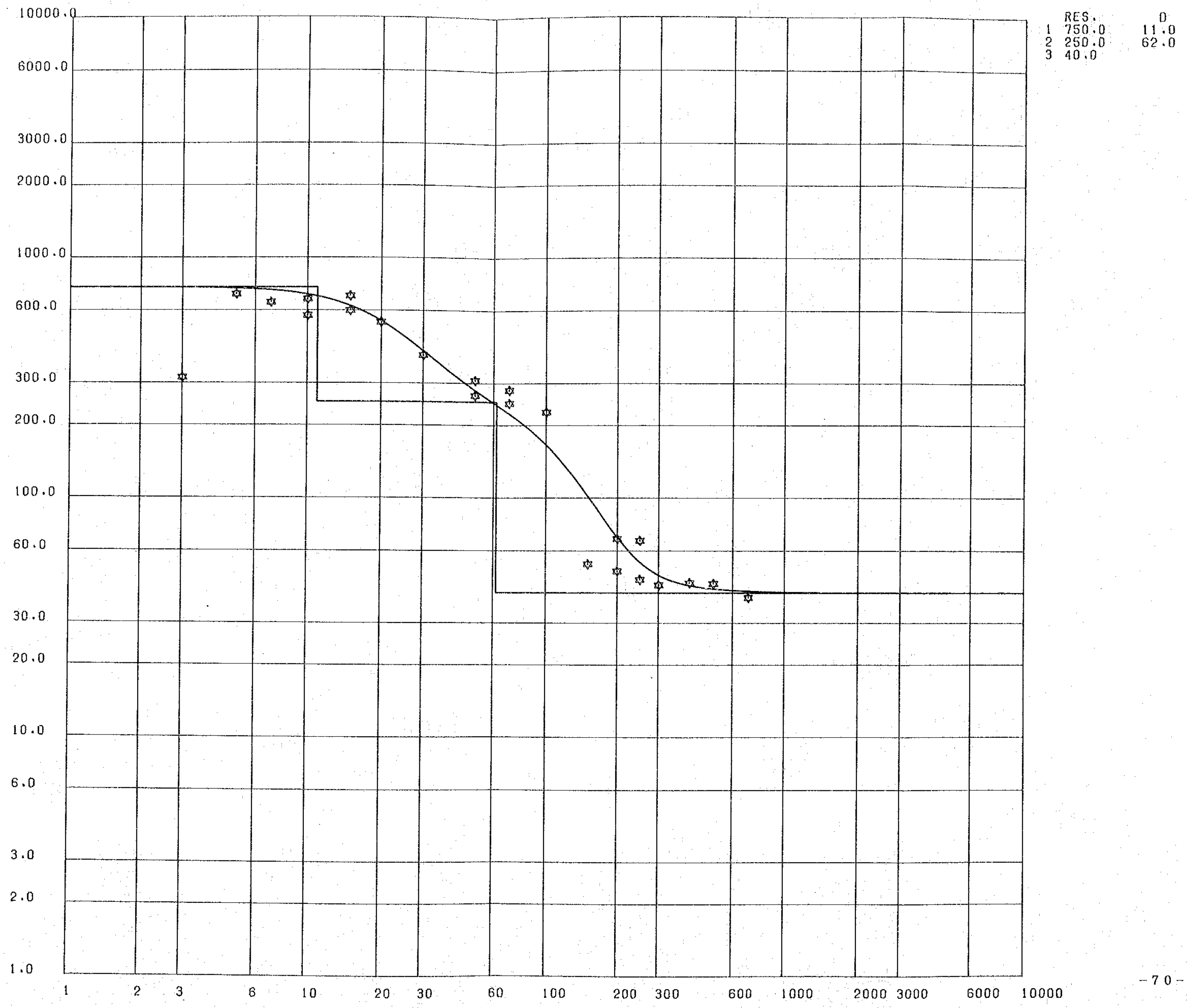

Fig IV − 4 (3)

VES Curve and Computer Model, Point E118

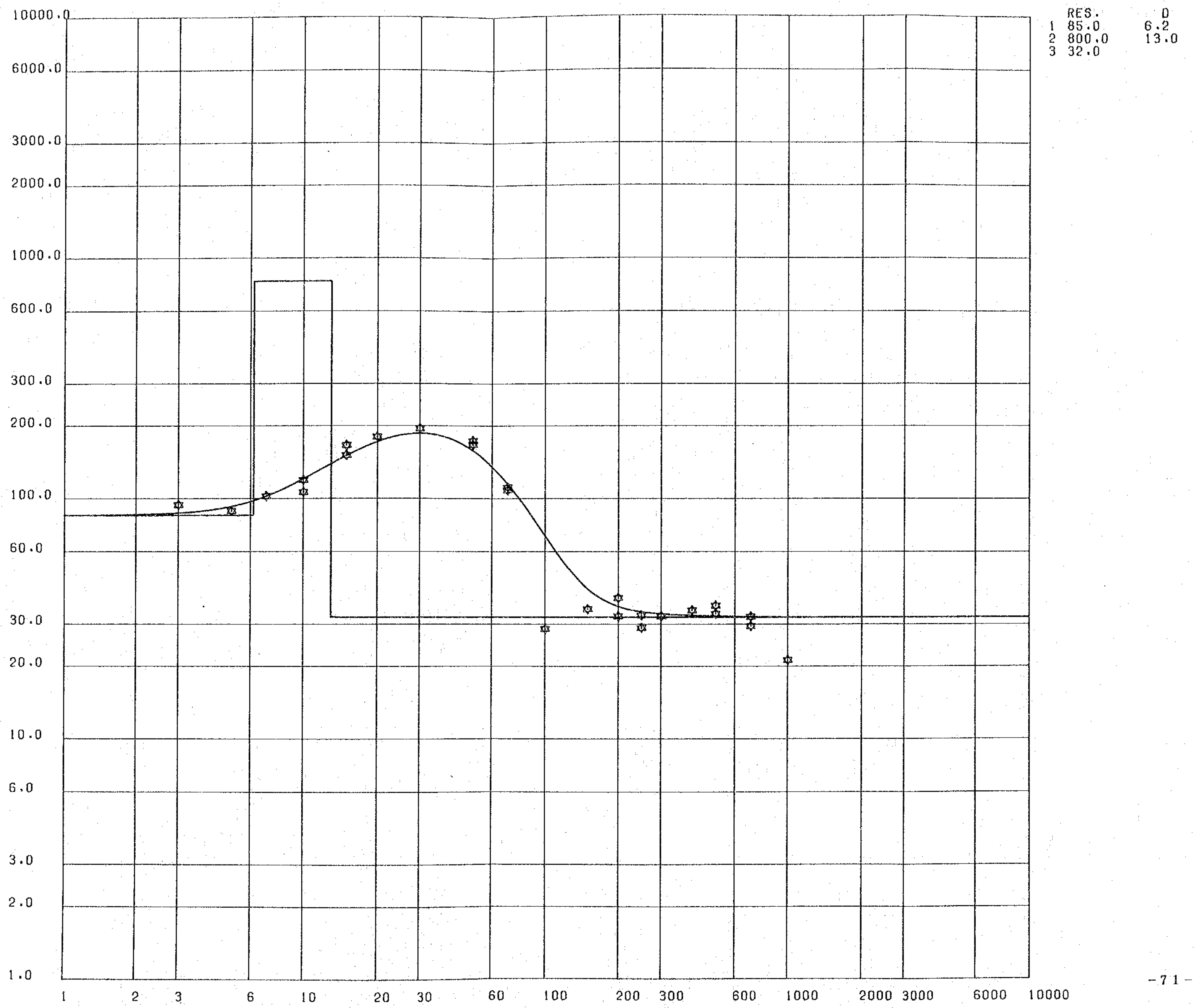

Fig IV — 4 (4)
VES Curve and Computer Model, Point E123

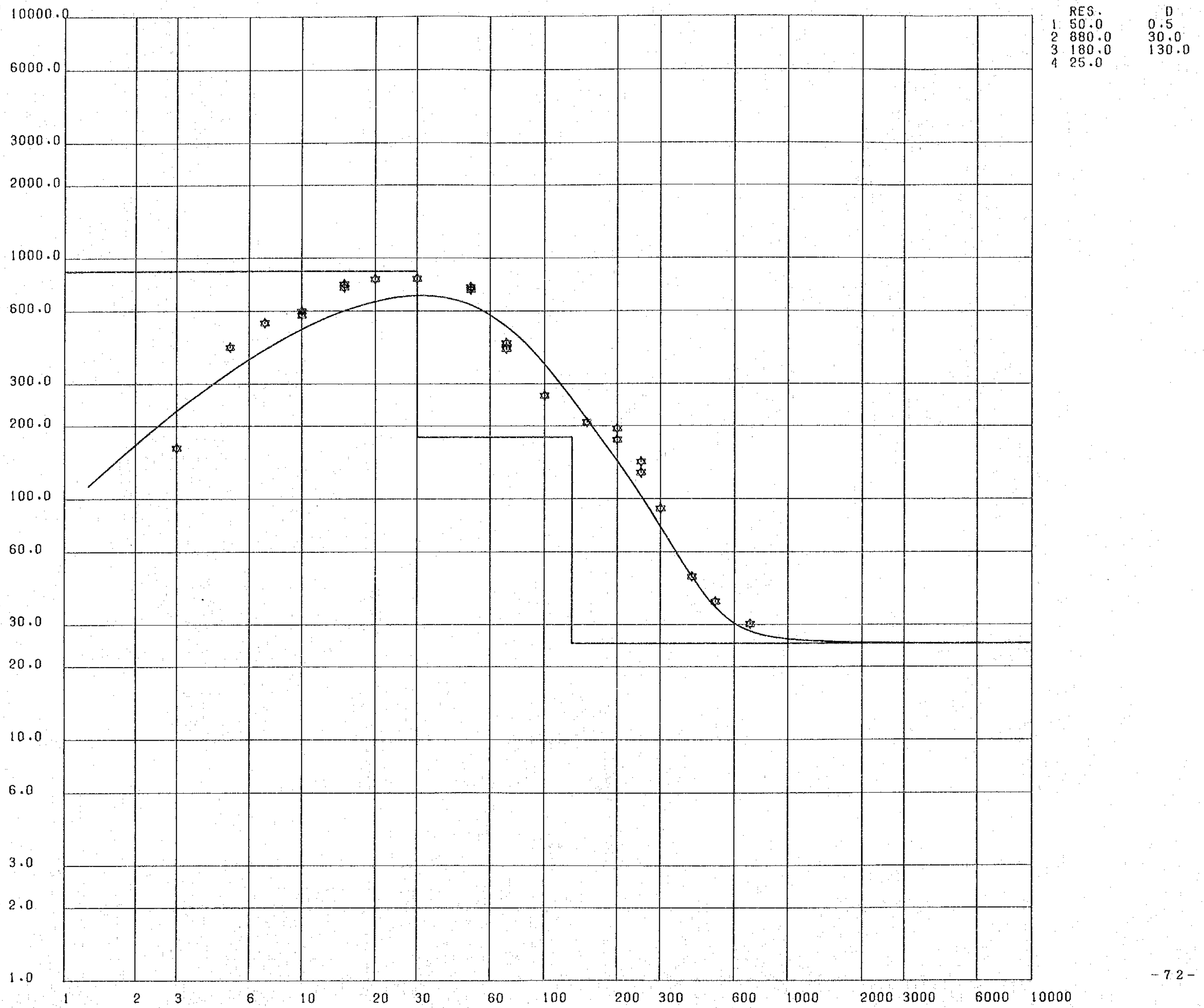

Fig Ⅳ — 4 (5)

VES Curve and Computer Model, Point E128

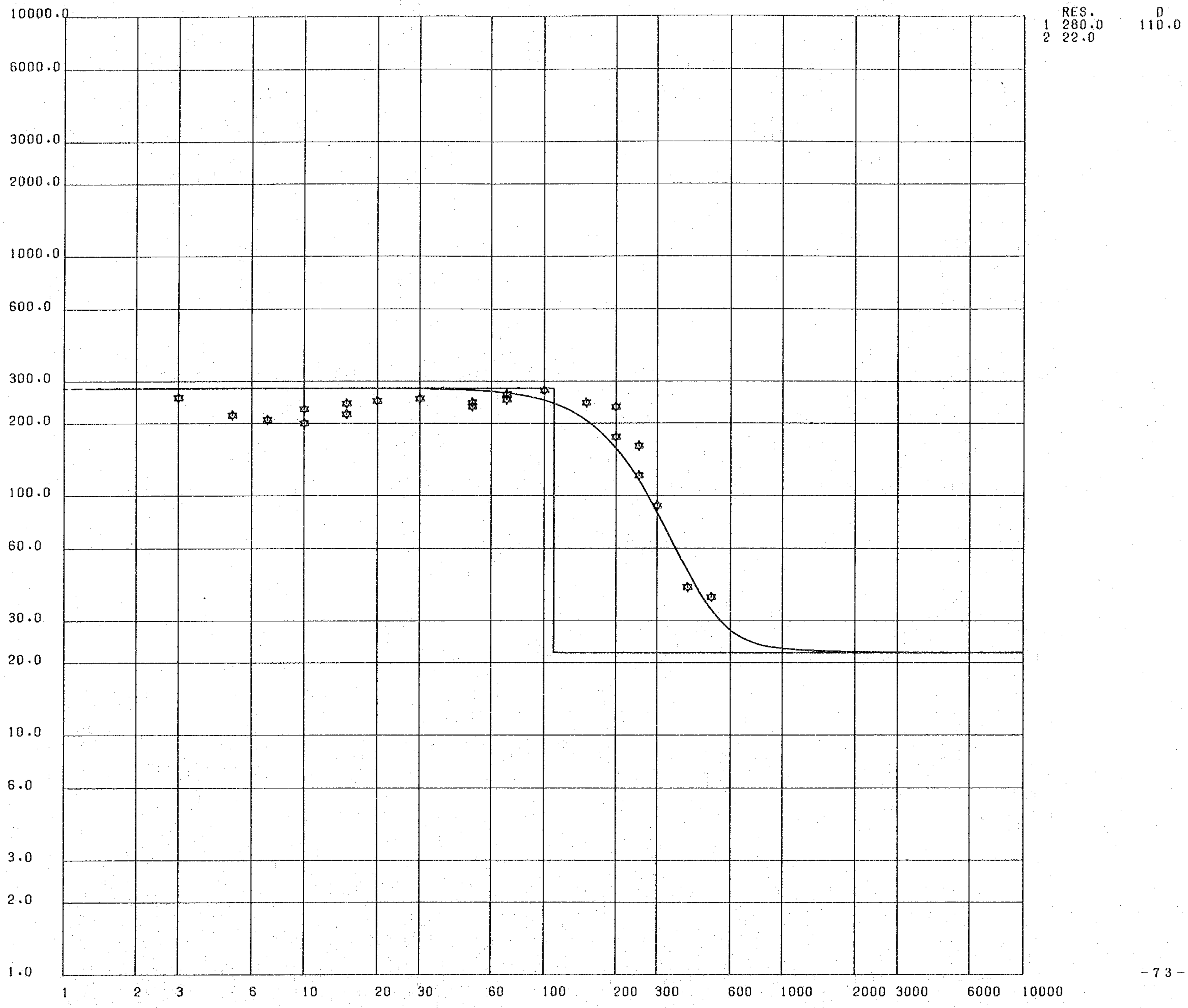

Fig IV — 4 (6)

VES Curve and Computer Model, Point H94

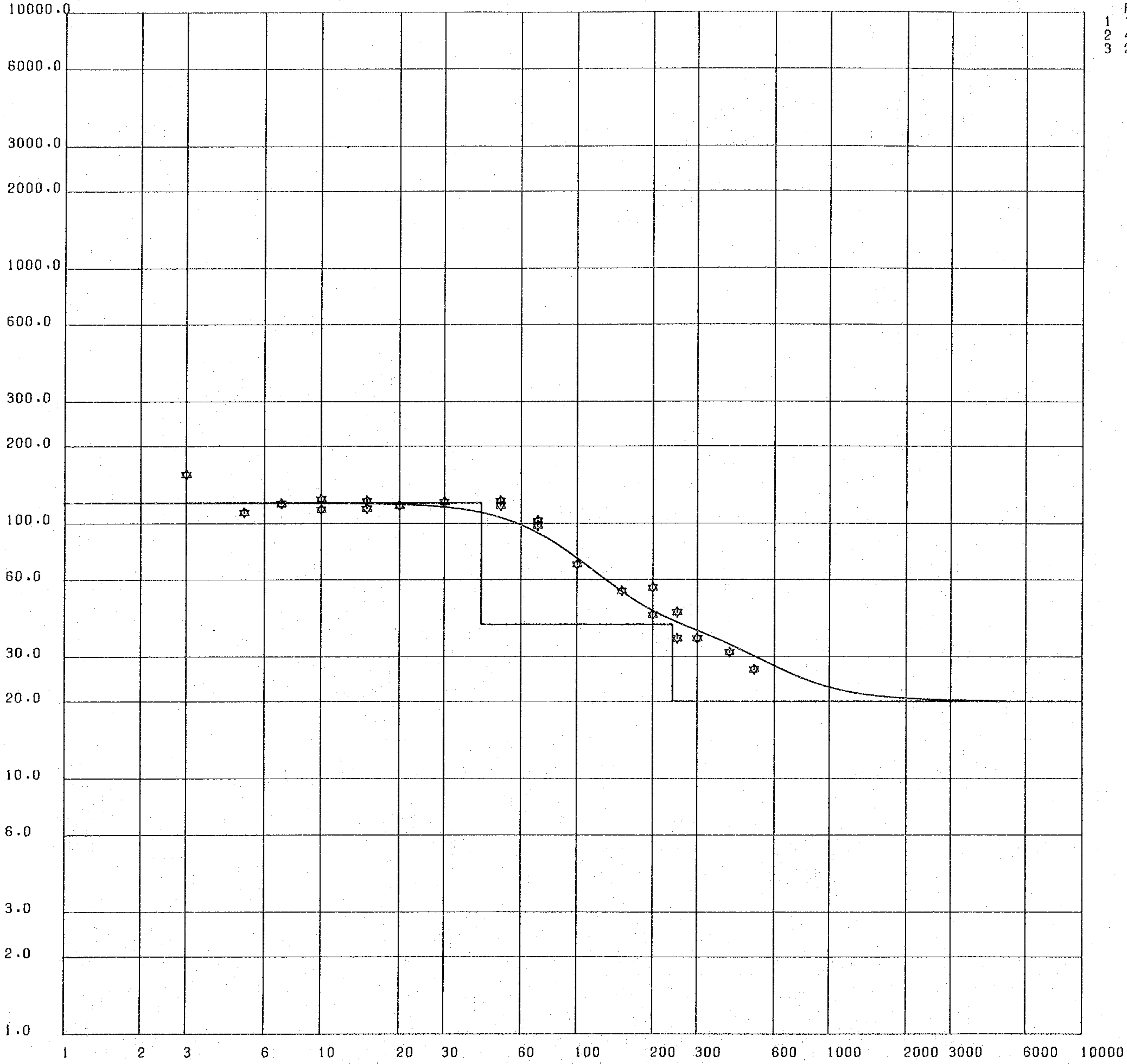

	RES.	D
1	120.0	42.0
2	40.0	240.0
3	20.0	

Fig IV — 4 (7)

VES Curve and Computer Model, Point H 99

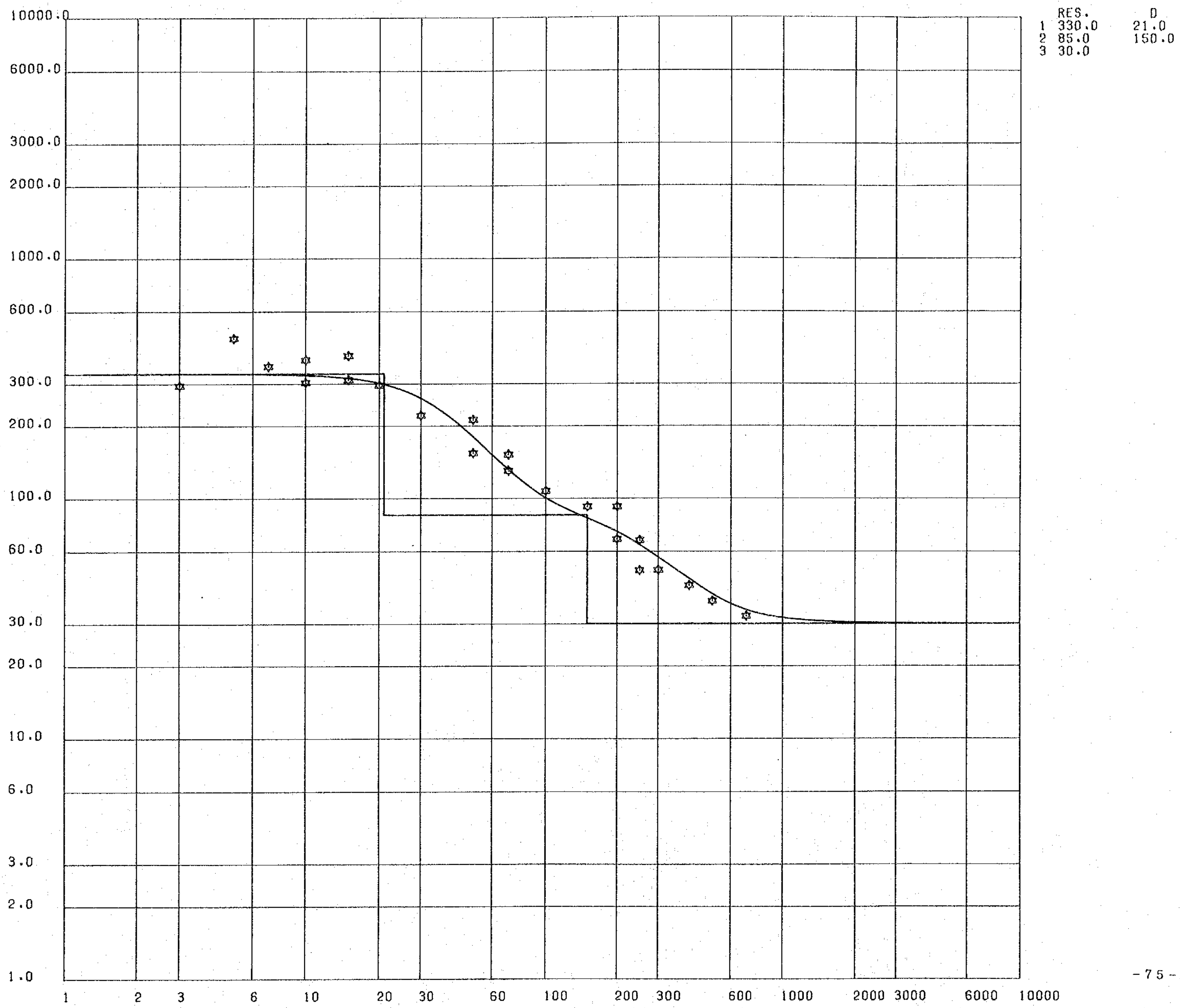

Fig IV — 4 (8)

VES Curve and Computer Model, Point H 104

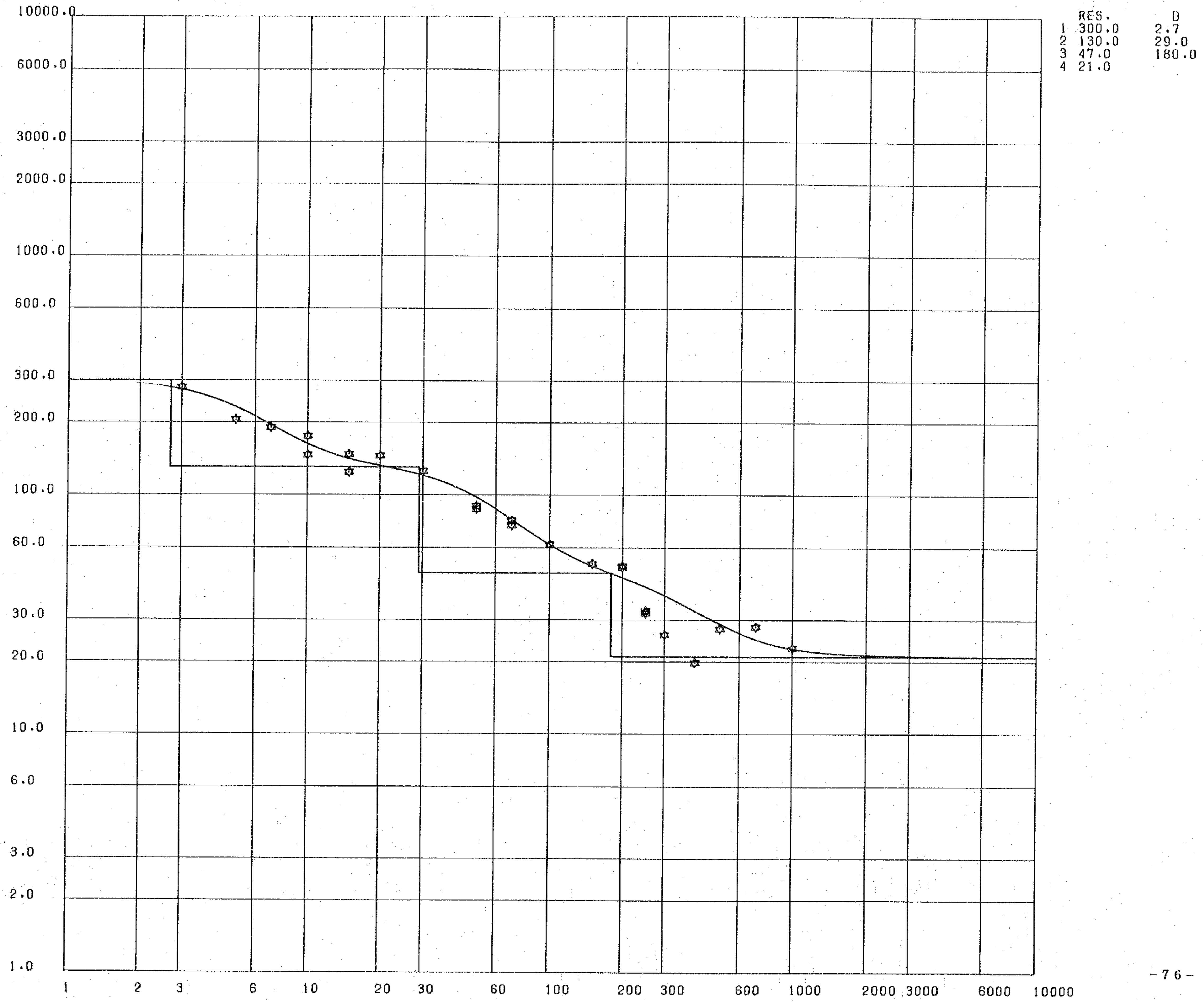

Fig IV-4 (9)

VES Curve and Computer Model, Point H109

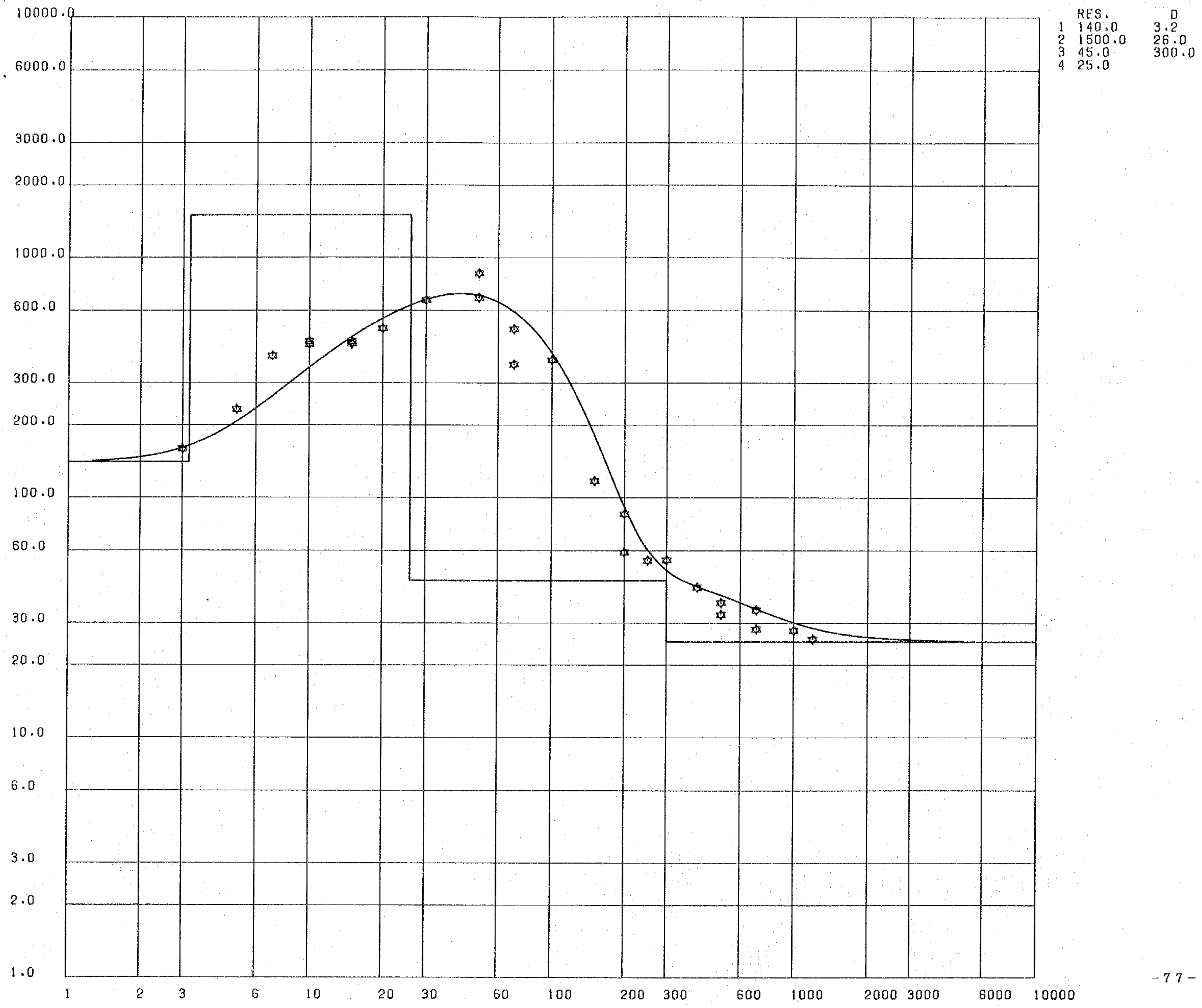

Fig IV — 4 (10)

VES Curve and Computer Model, Point H114

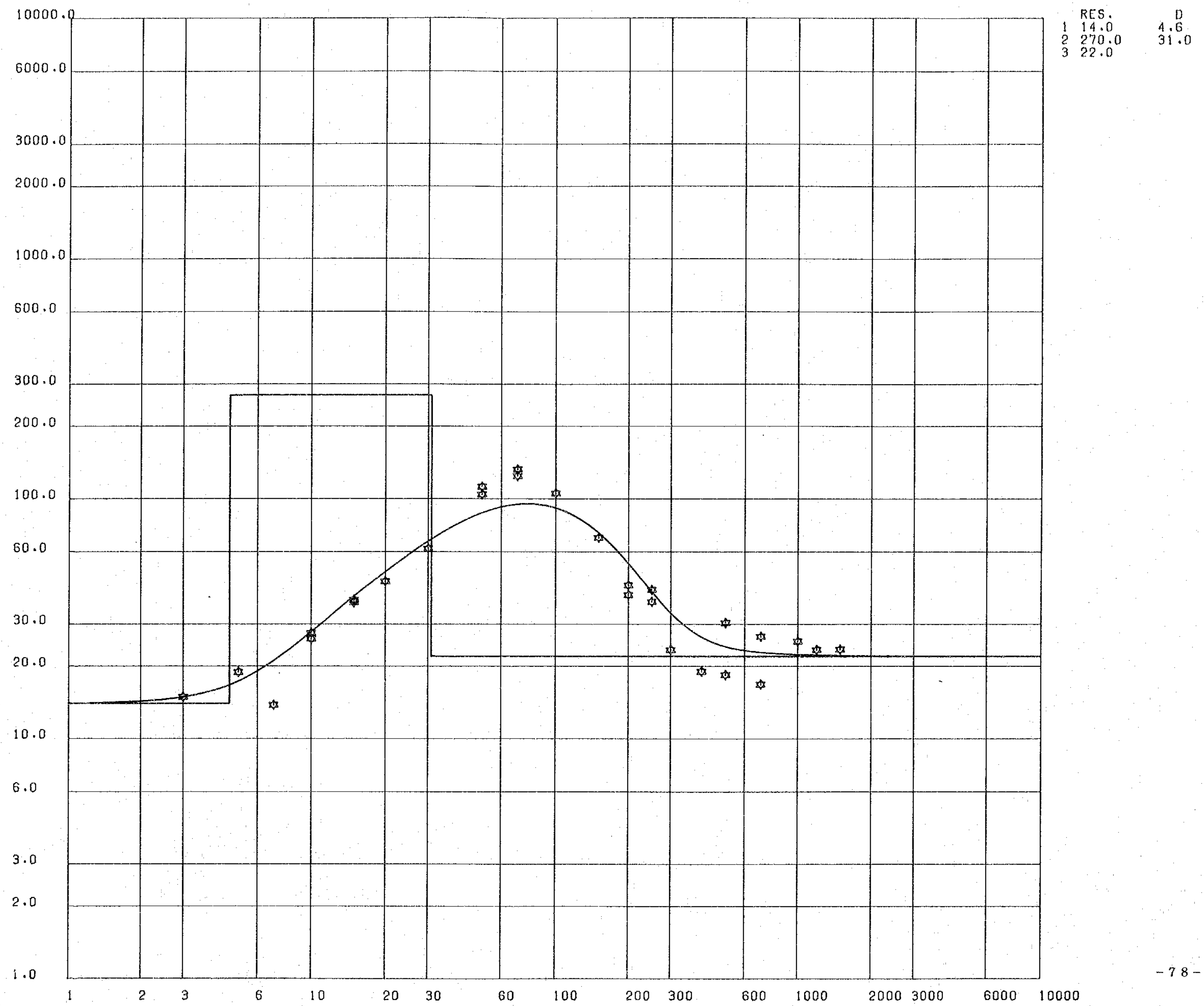

Fig IV-4 (II)

VES Curve and Computer Model, Point H120

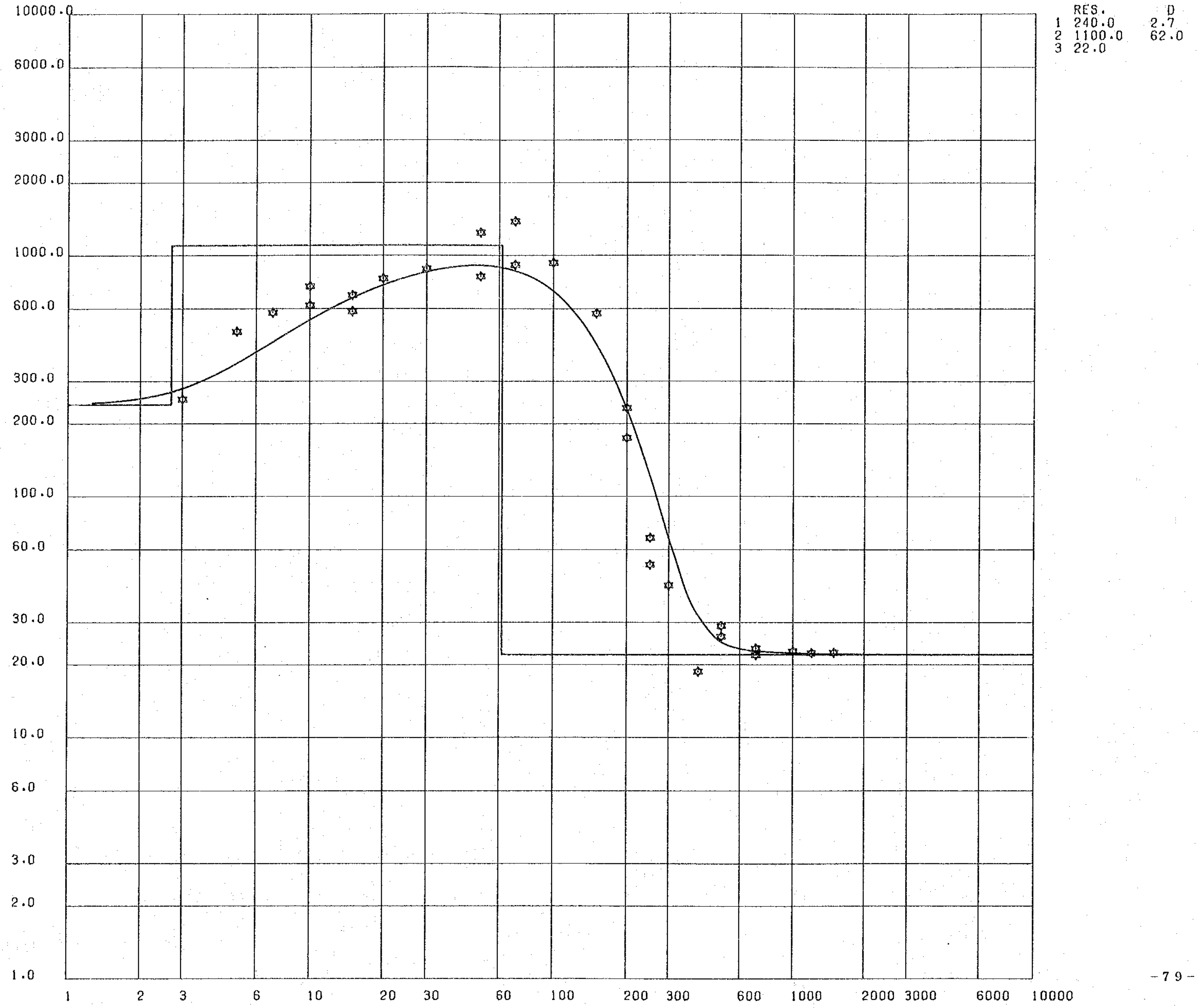

Fig Ⅳ－4 (12)

VES Curve and Computer Model, Point H 124

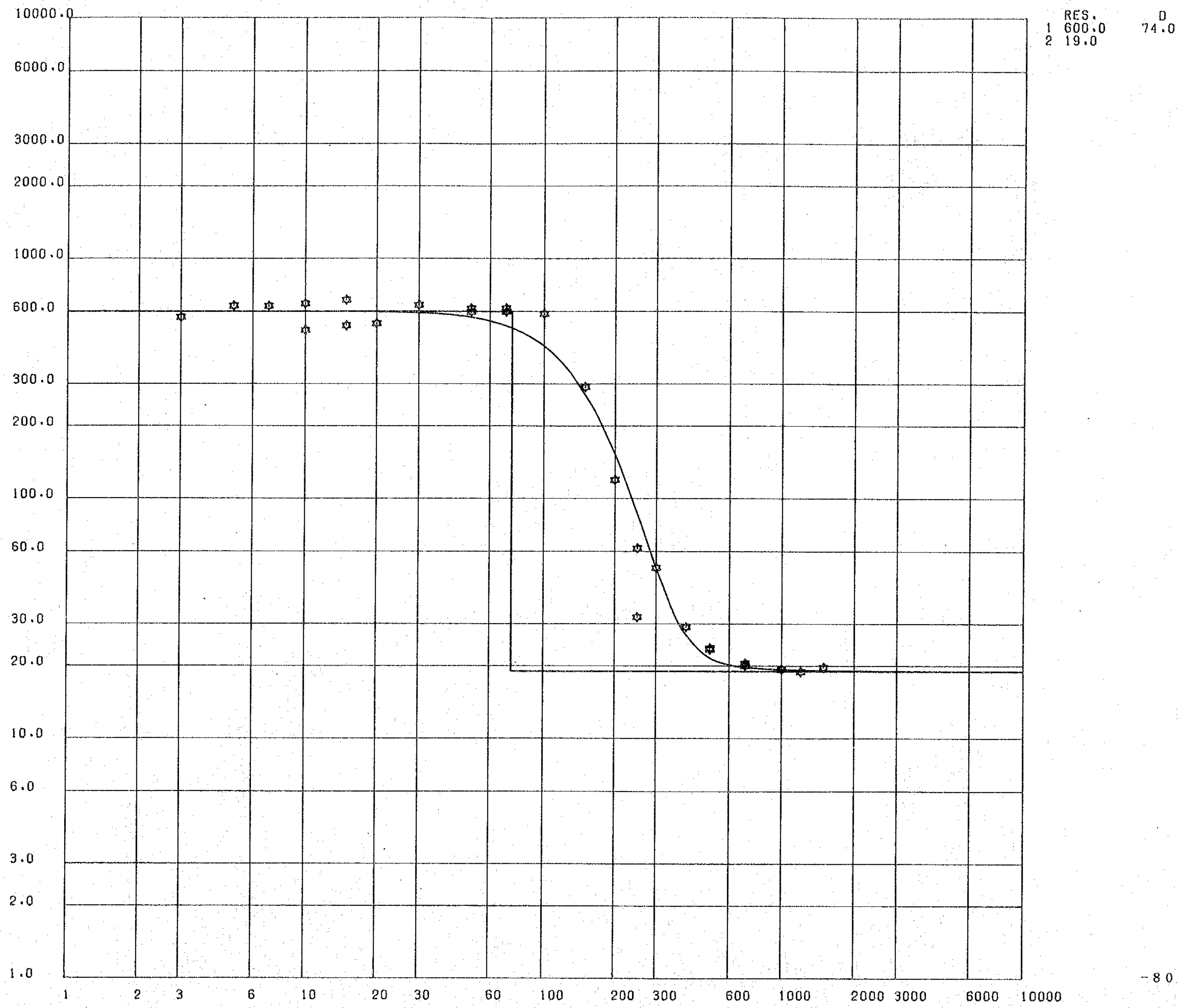

Fig IV-4 (13)

VES Curve and Computer Model, Point H129

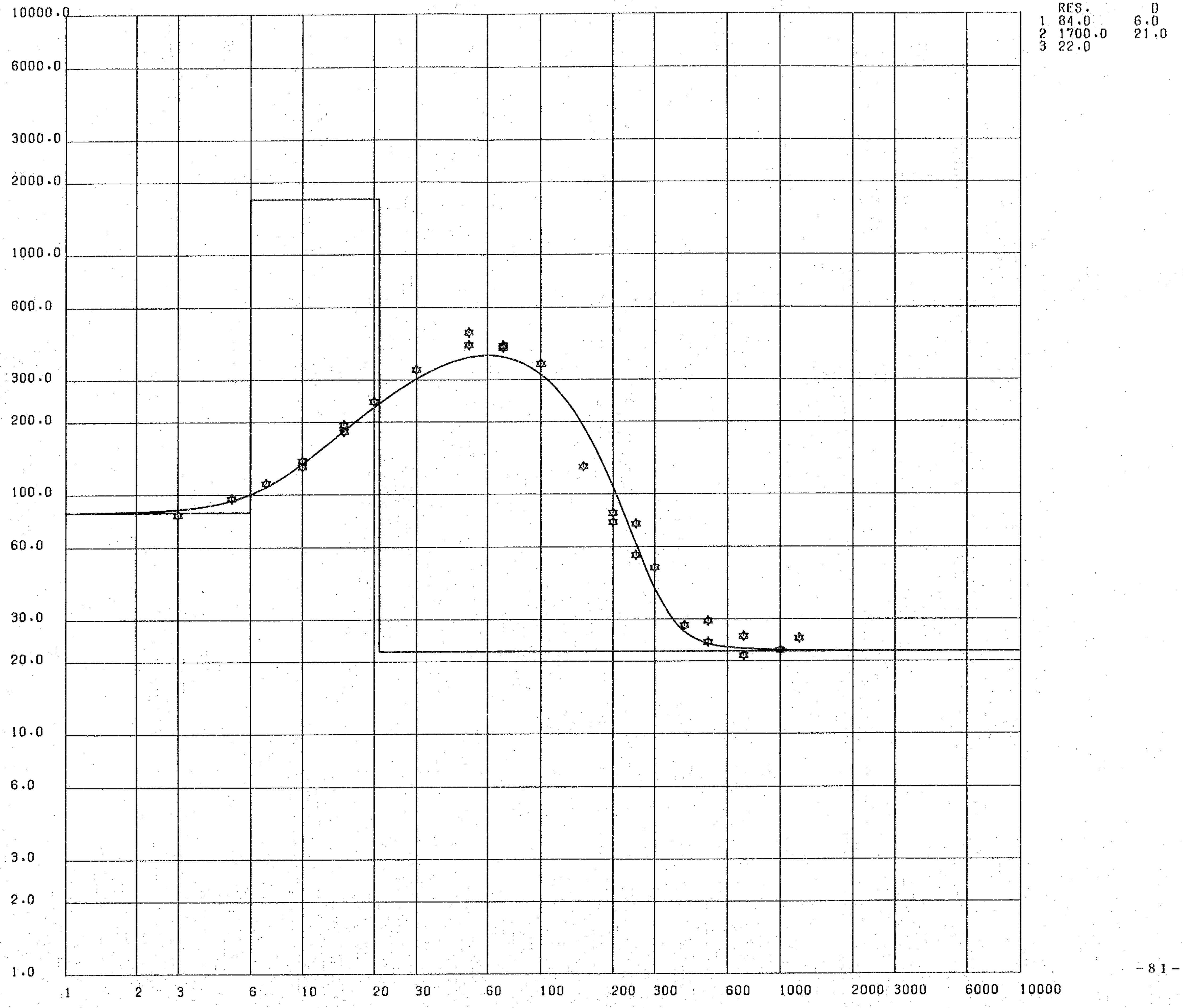

Fig IV − 4 (14)

VES Curve and Computer Model, Point H134

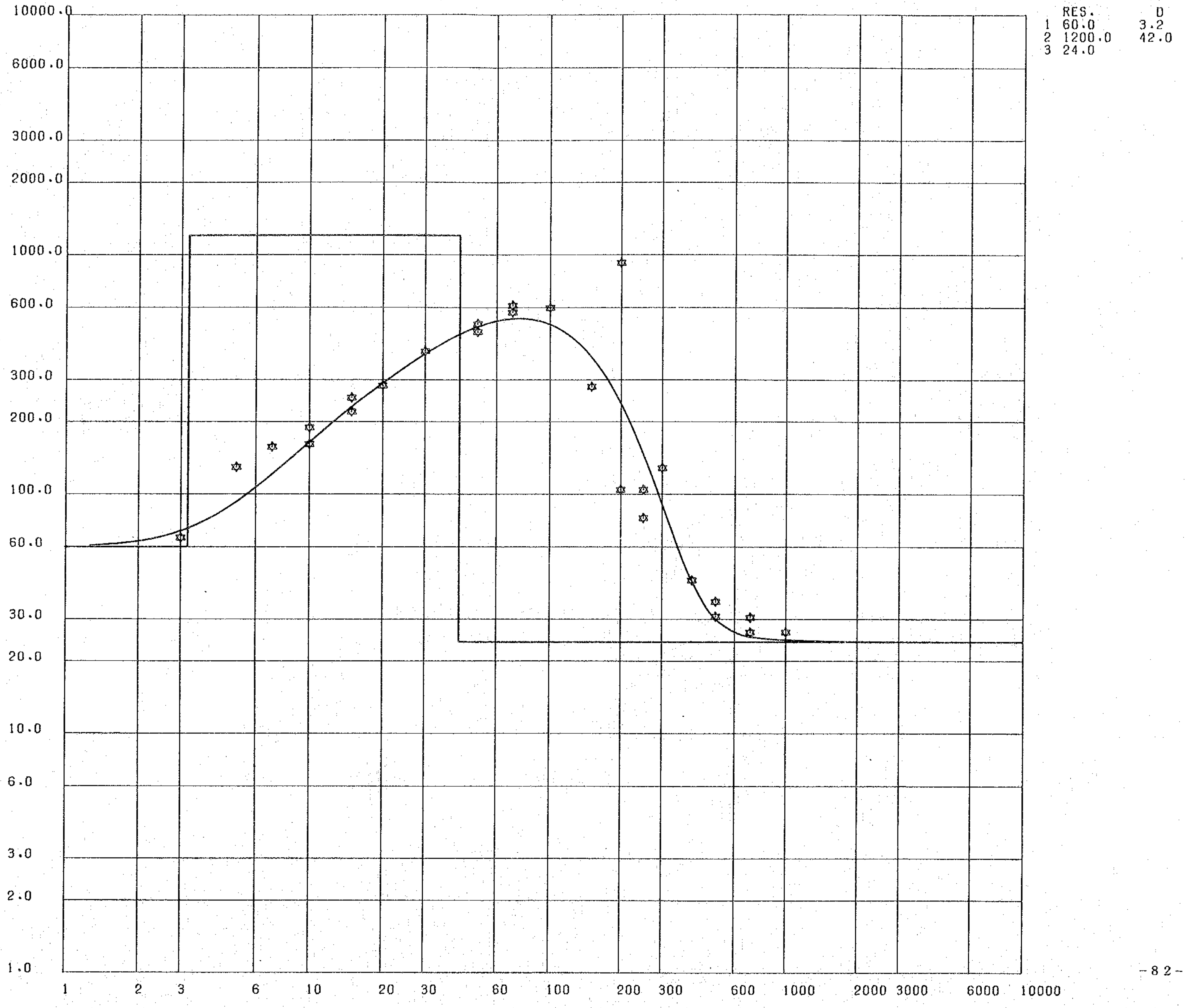

Fig IV-4(15)

VES Curve and Computer Model, Point H 139

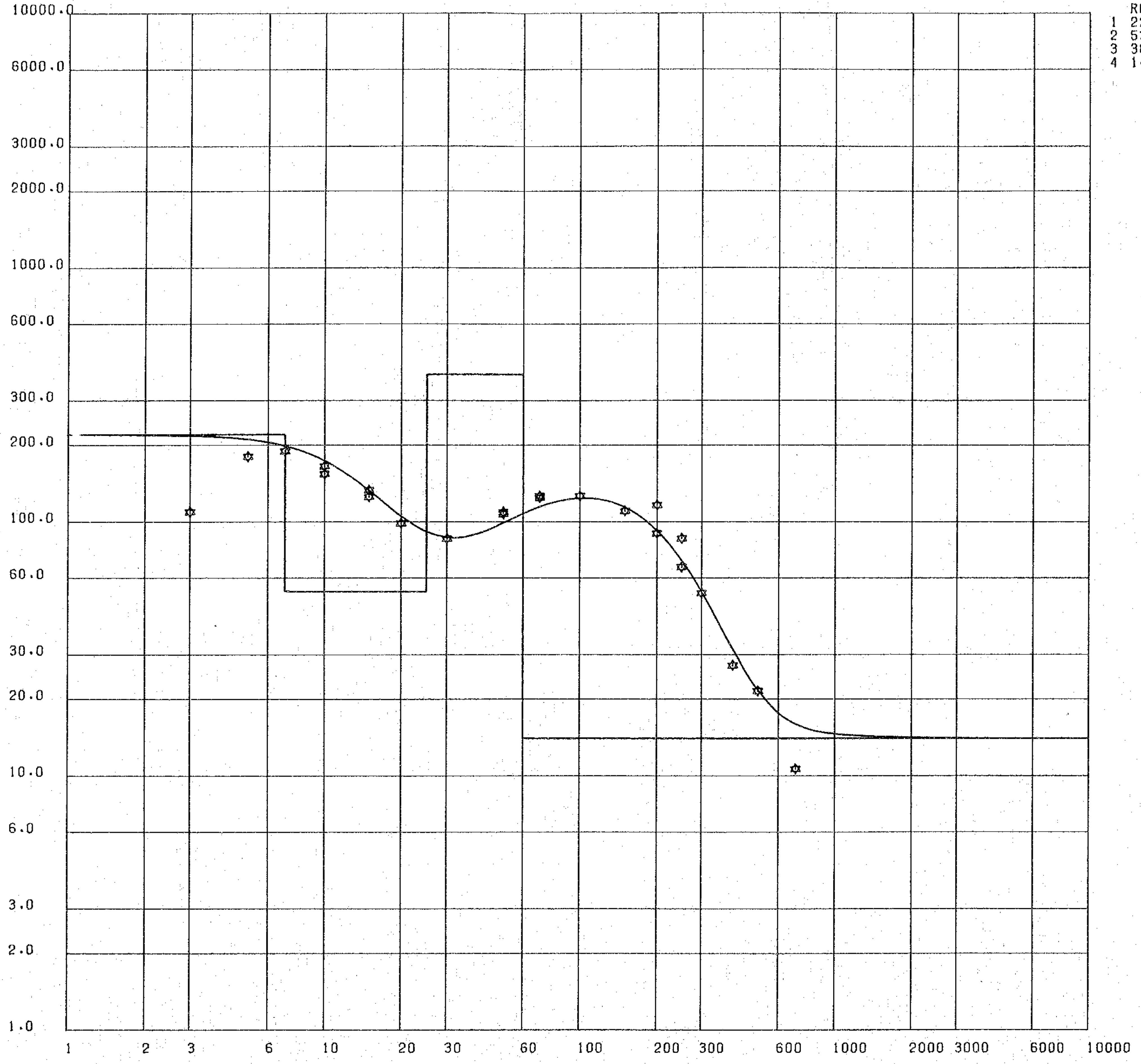

	RES.	D
1	220.0	7.0
2	53.0	25.0
3	380.0	60.0
4	14.0	

Fig IV-4(16)

VES Curve and Computer Model, Point K101

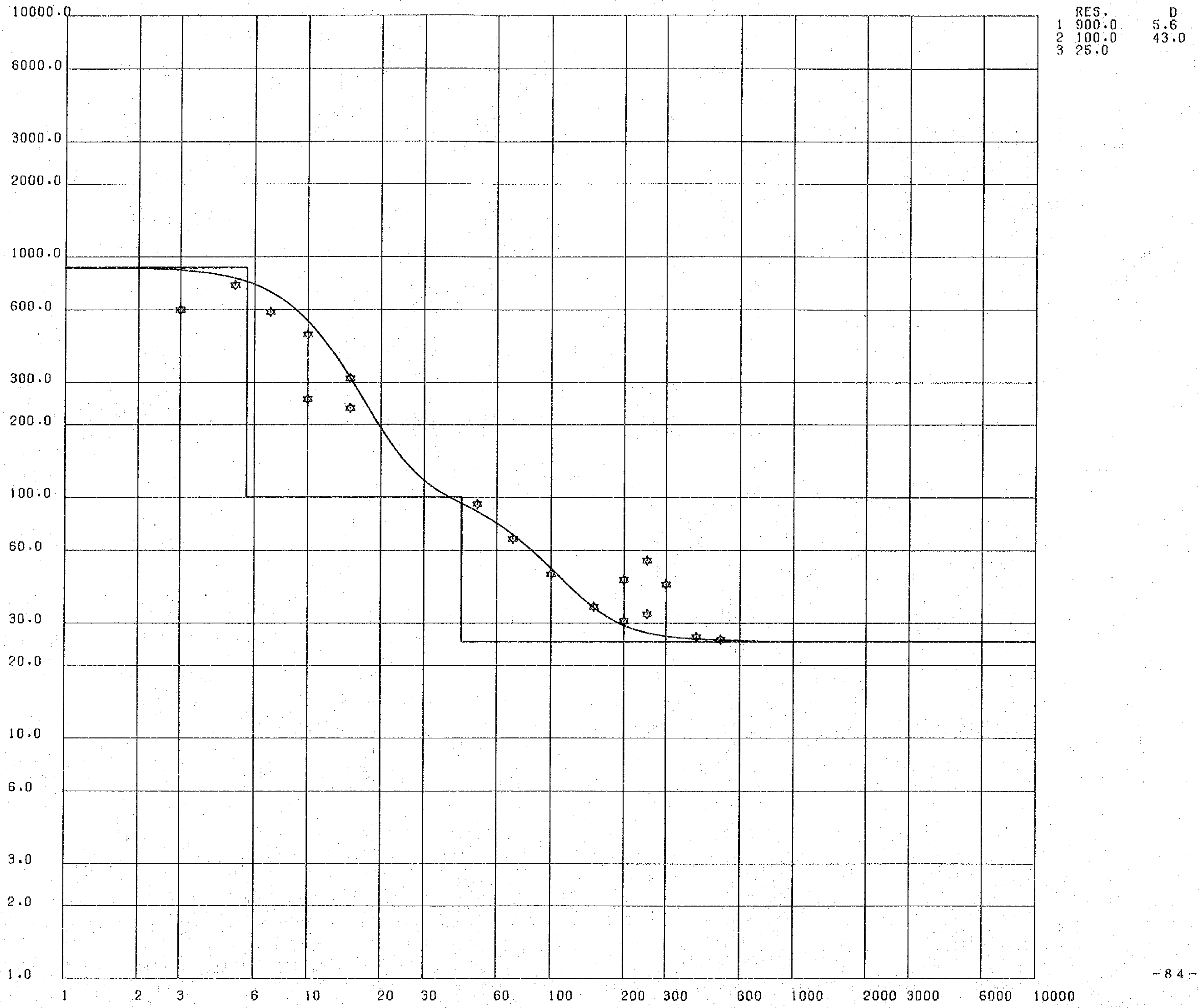

Fig Ⅳ－4 (17)

VES Curve and Computer Model, Point K 106

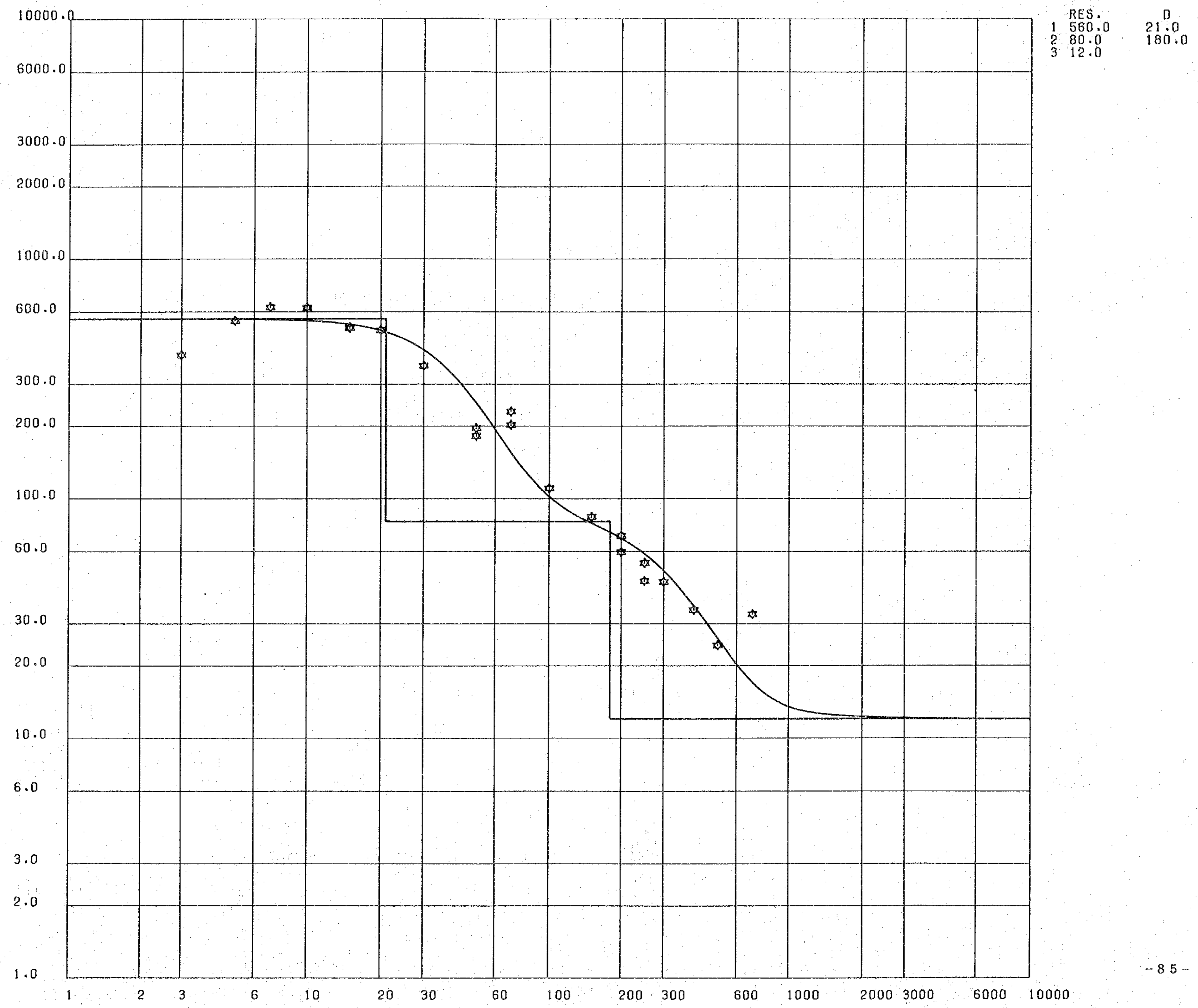

Fig IV-4(18)

VES Curve and Computer Model, Point KIII

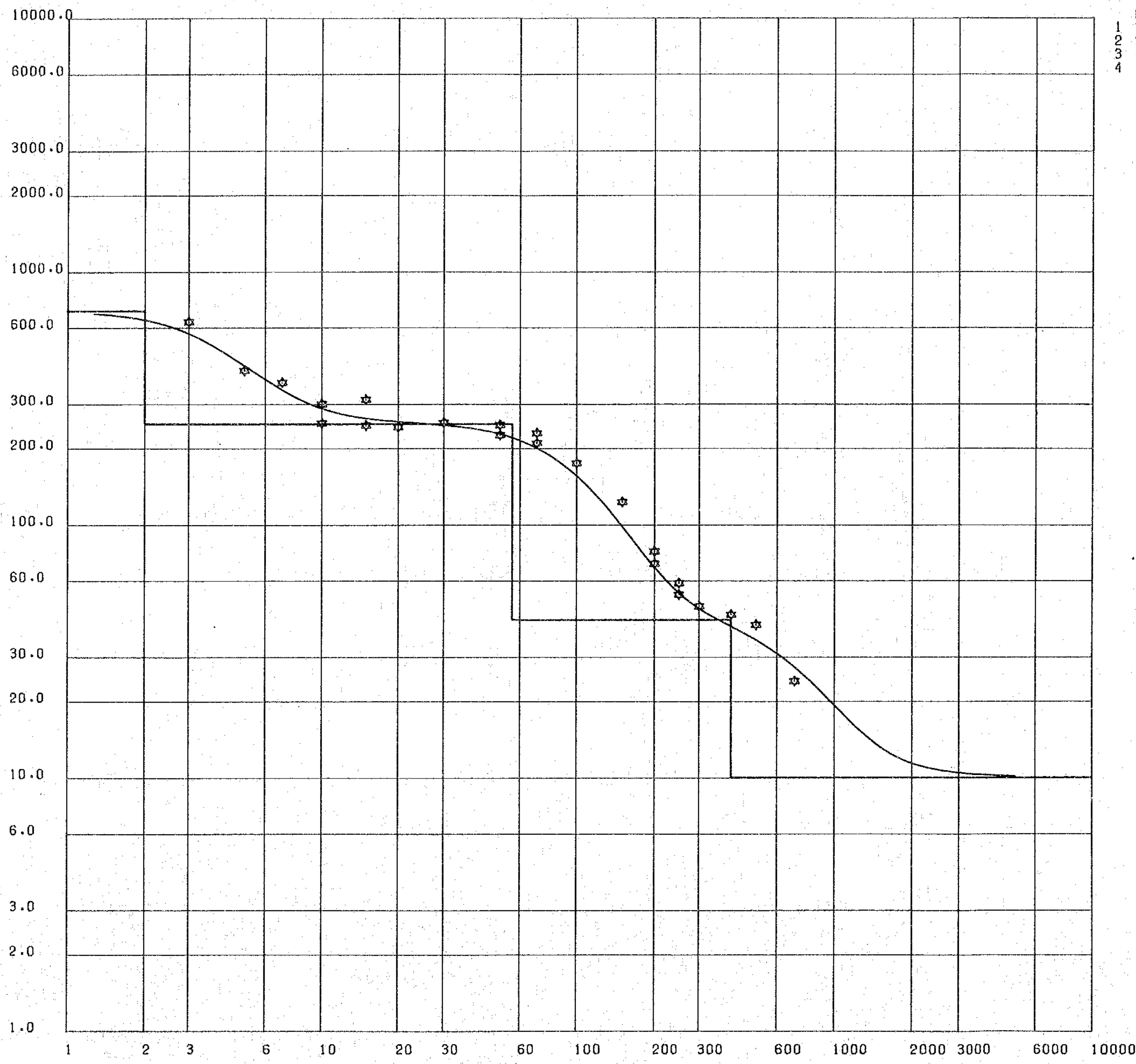

	RES.	D
1	700.0	2.0
2	250.0	56.0
3	42.0	400.0
4	10.0	

Fig IV—4(19)

VES Curve and Computer Model, Point K116

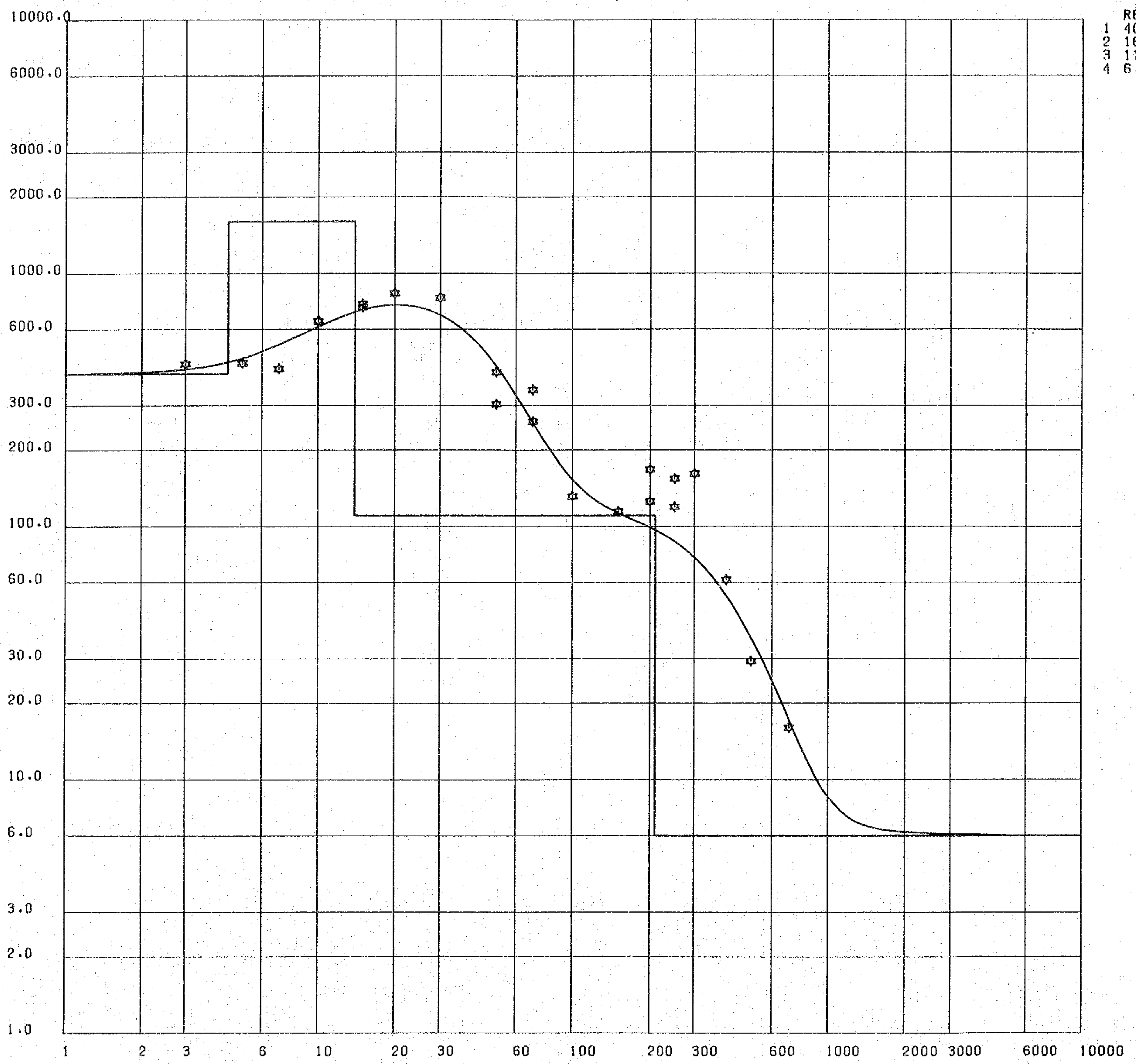

	RES.	D
1	400.0	4.4
2	1600.0	14.0
3	110.0	210.0
4	6.0	

Fig Ⅳ—4 (20)

VES Curve and Computer Model, Point K121

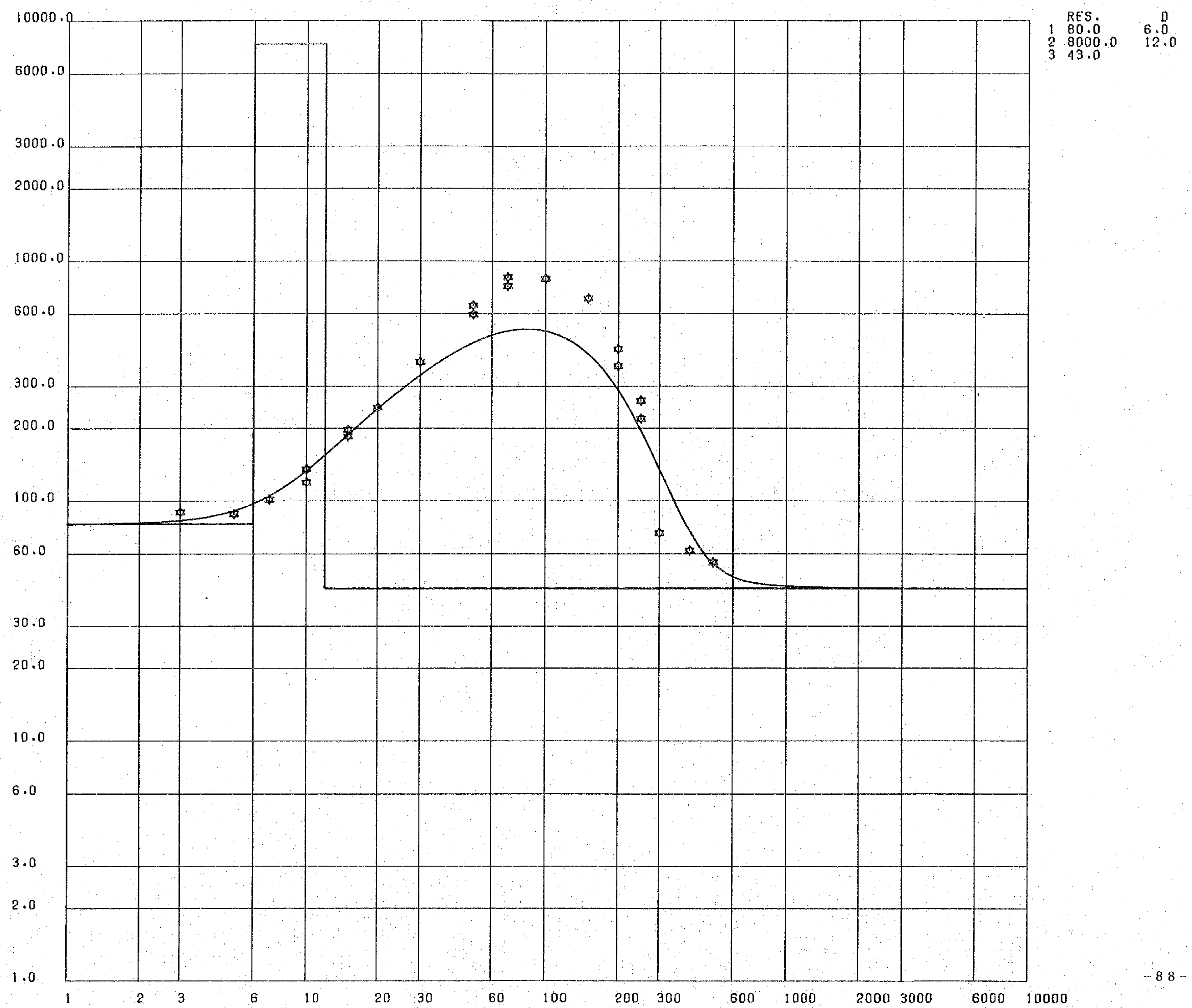

Fig Ⅳ-4(21)

VES Curve and Computer Model, Point M80

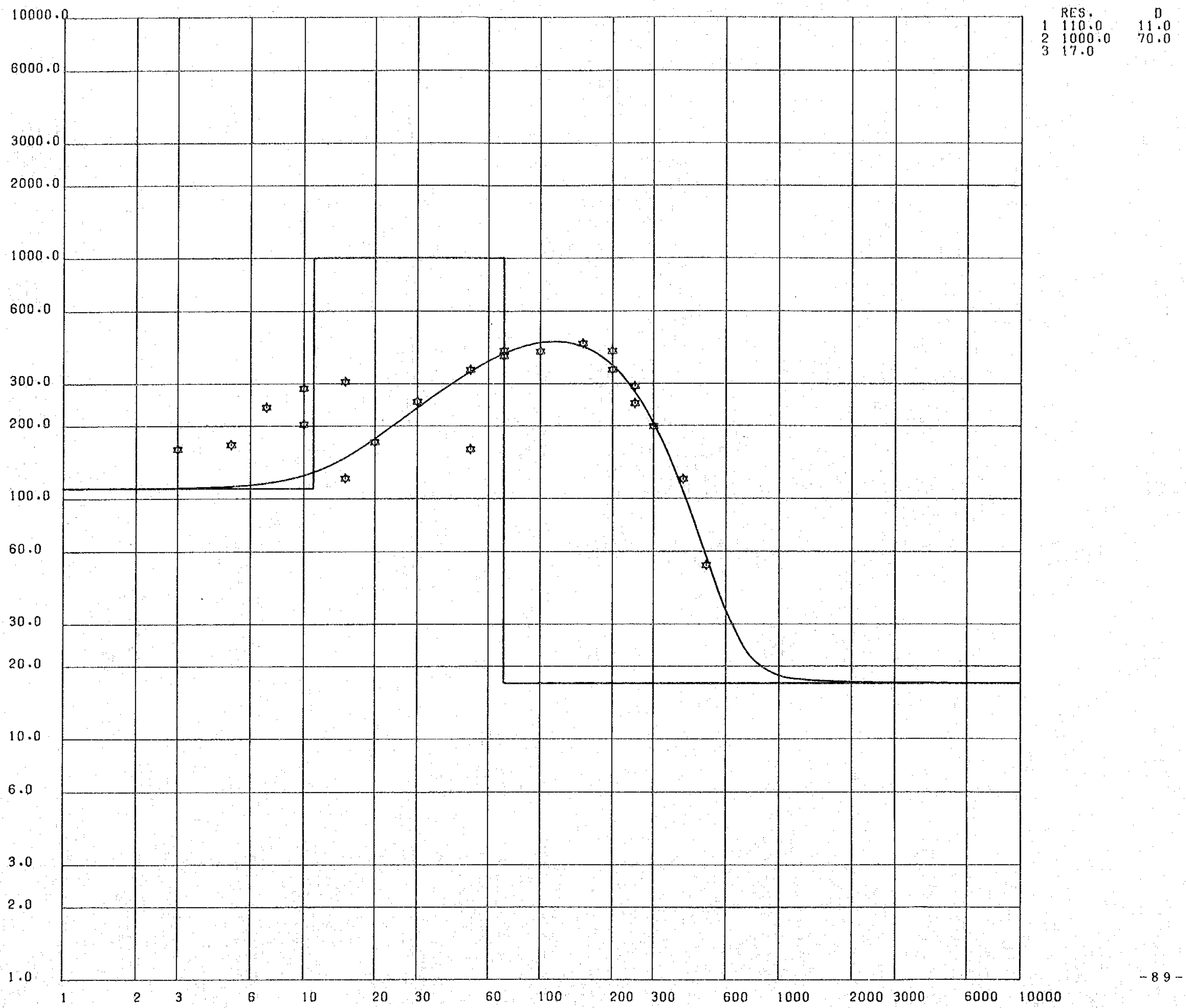

Fig Ⅳ－4(22)

VES Curve and Computer Model, Point M85

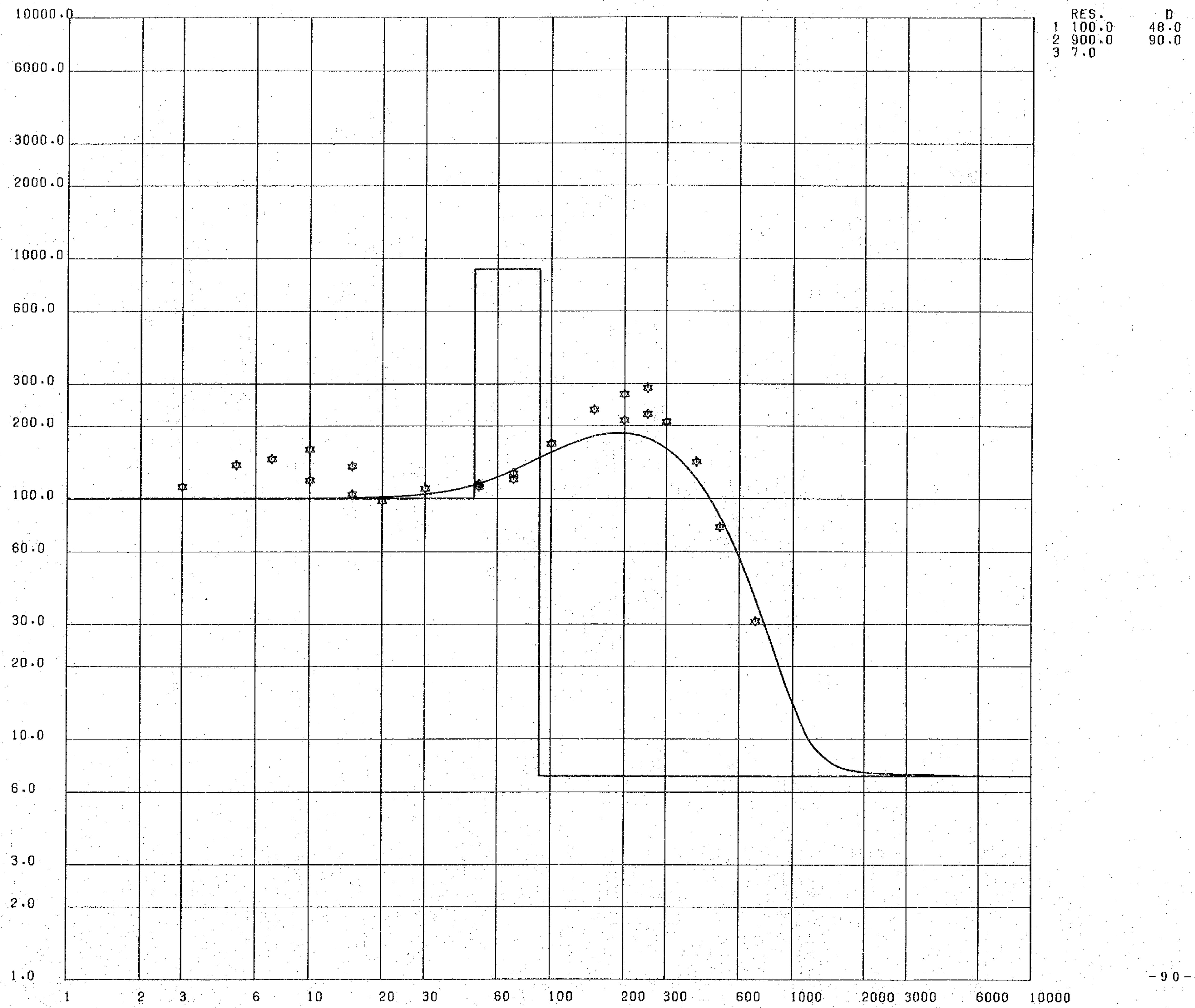

Fig Ⅳ－4 (23)

VES Curve and Computer Model, Point M90

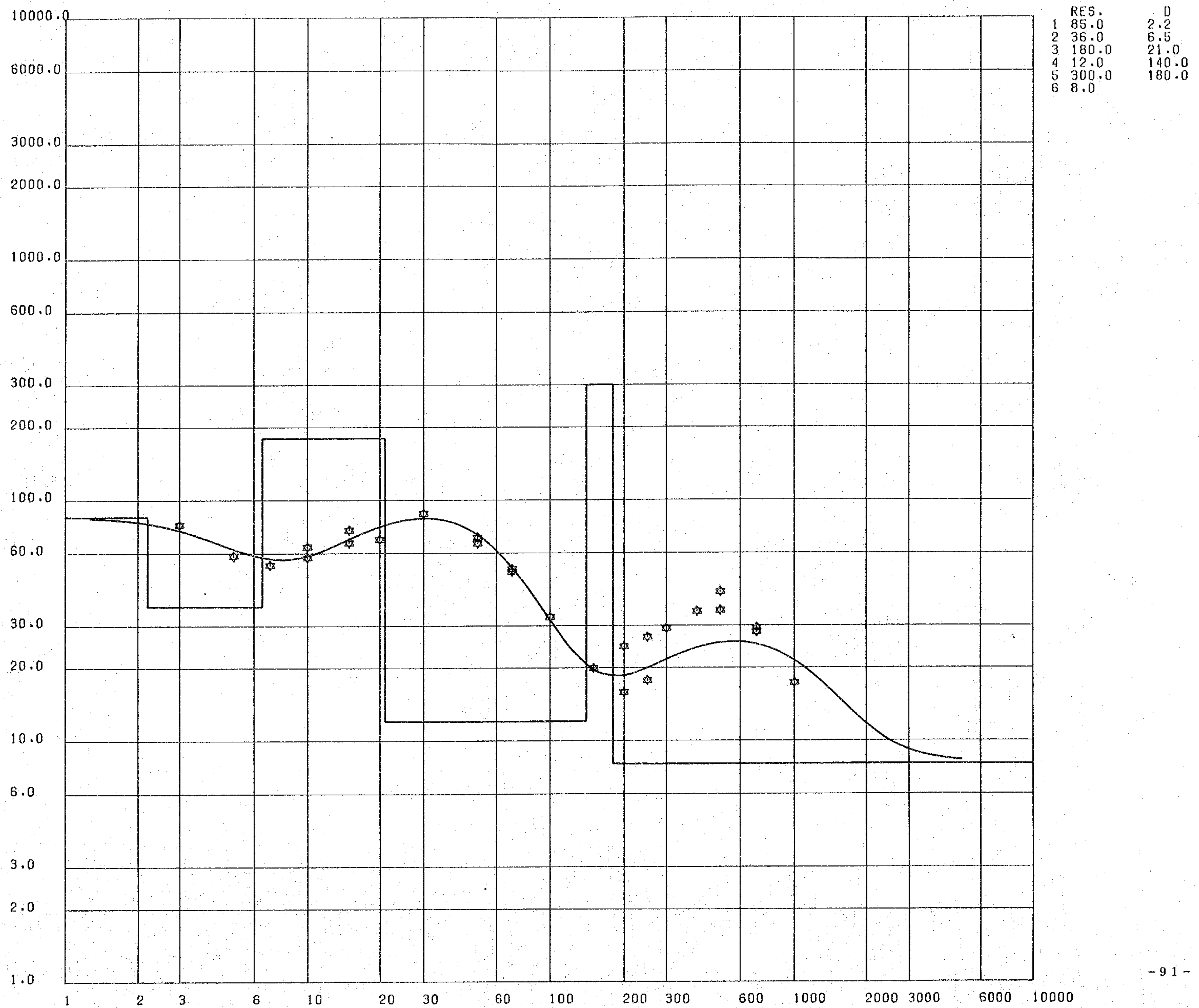

Fig Ⅳ－4(24)

VES Curve and Computer Model, Point M95

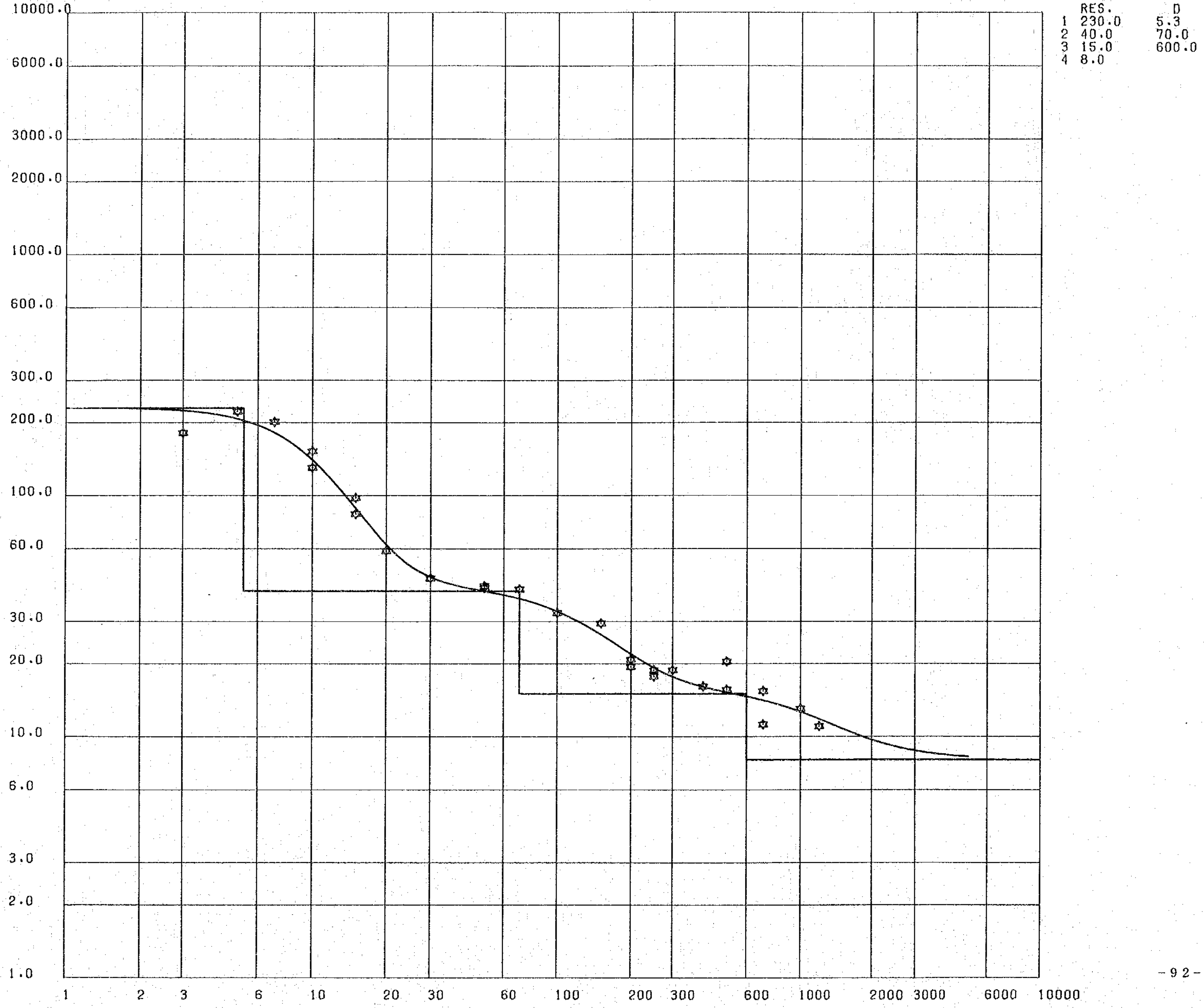

Fig Ⅳ— 4(25)

VES Curve and Computer Model, Point M 100

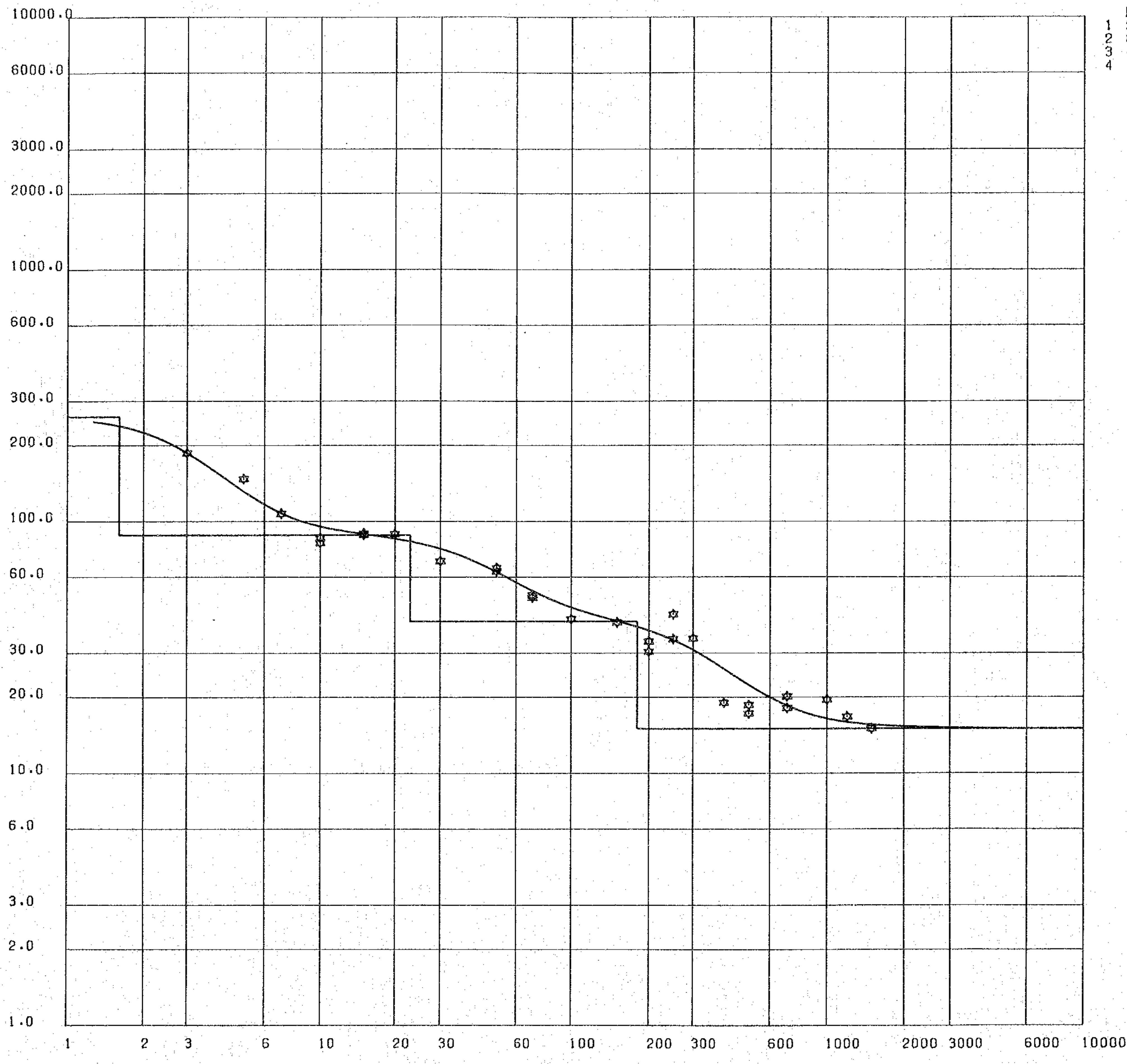

	RES.	D
1	260.0	1.6
2	88.0	23.0
3	40.0	180.0
4	15.0	

Fig Ⅳ－4(26)

VES Curve and Computer Model, Point M105

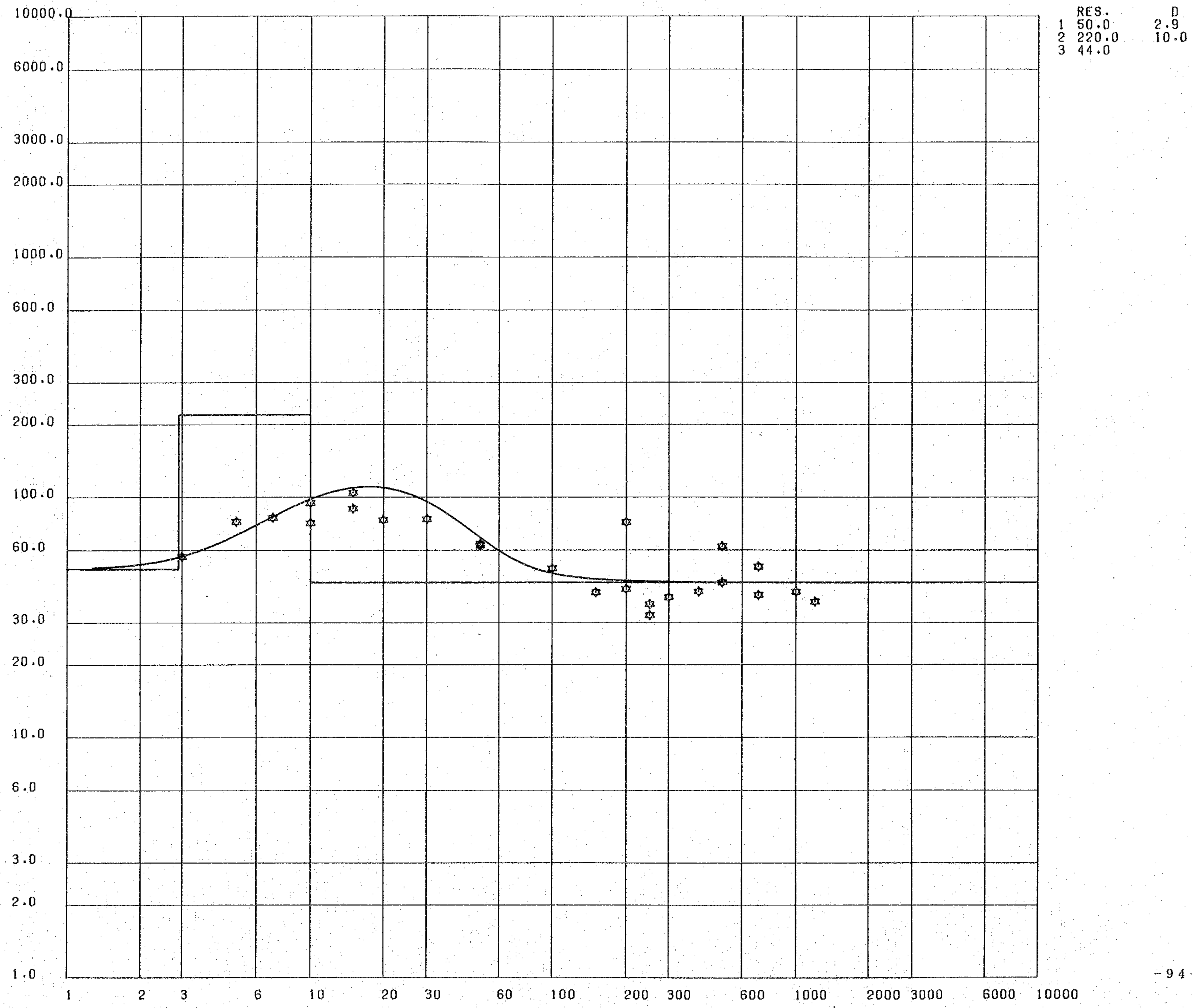

Fig Ⅳ－4(27)

VES Curve and Computer Model, Point M110

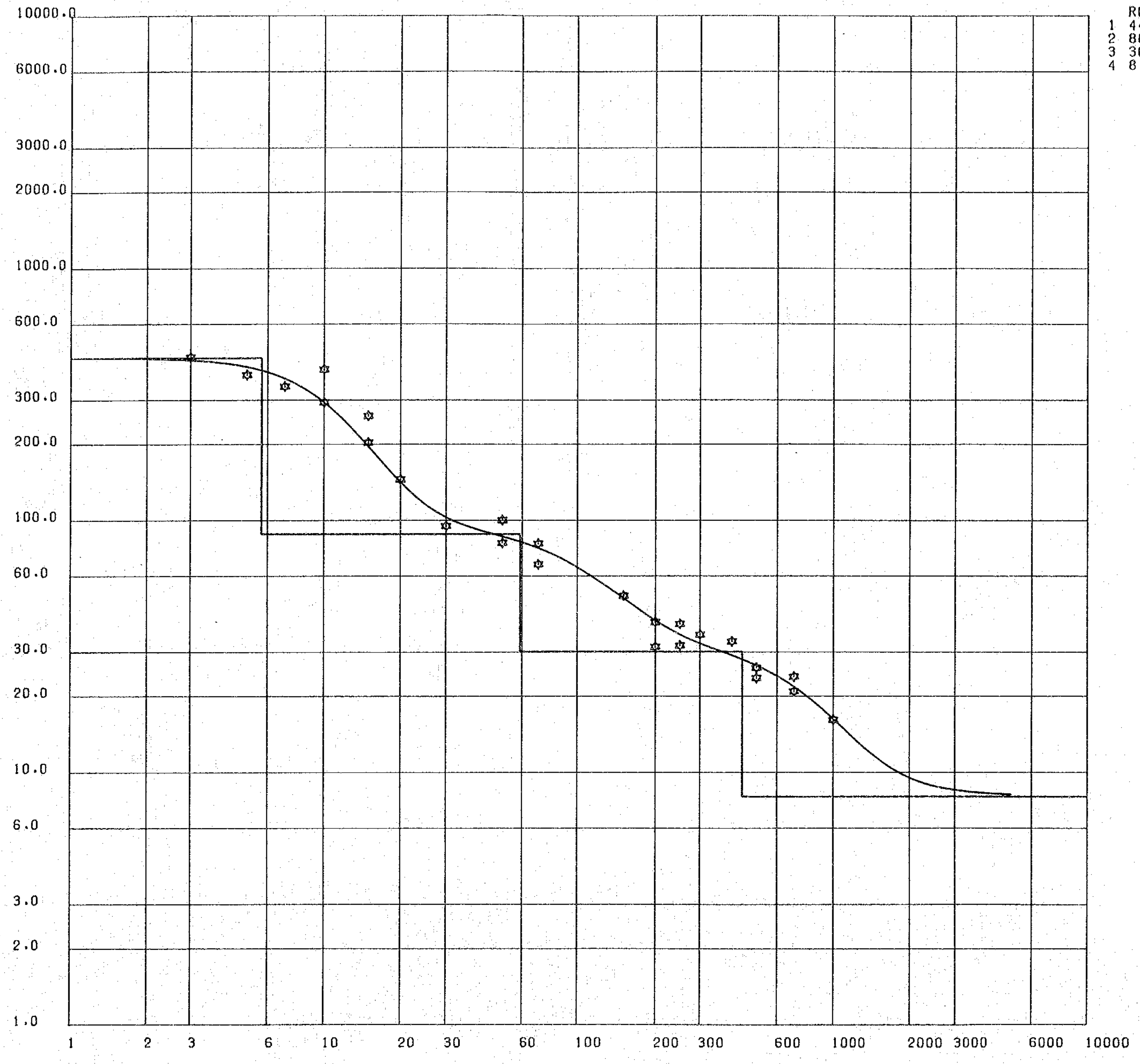

	RES.	D
1	440.0	5.7
2	88.0	59.0
3	30.0	440.0
4	8.0	

Fig Ⅳ－4(28)

VES Curve and Computer Model, Point M115

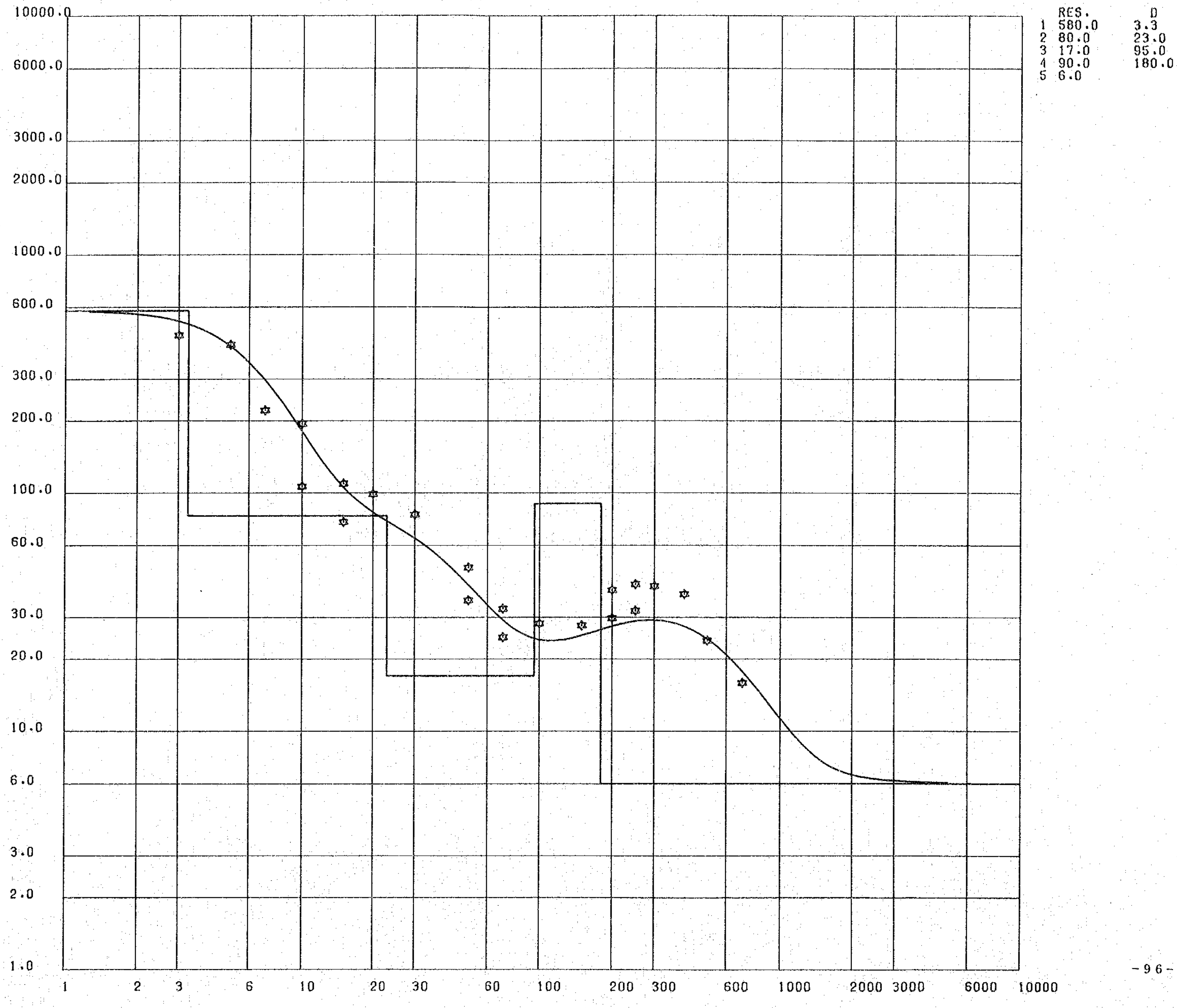

Fig IV-4(29)

VES Curve and Computer Model, Point M120

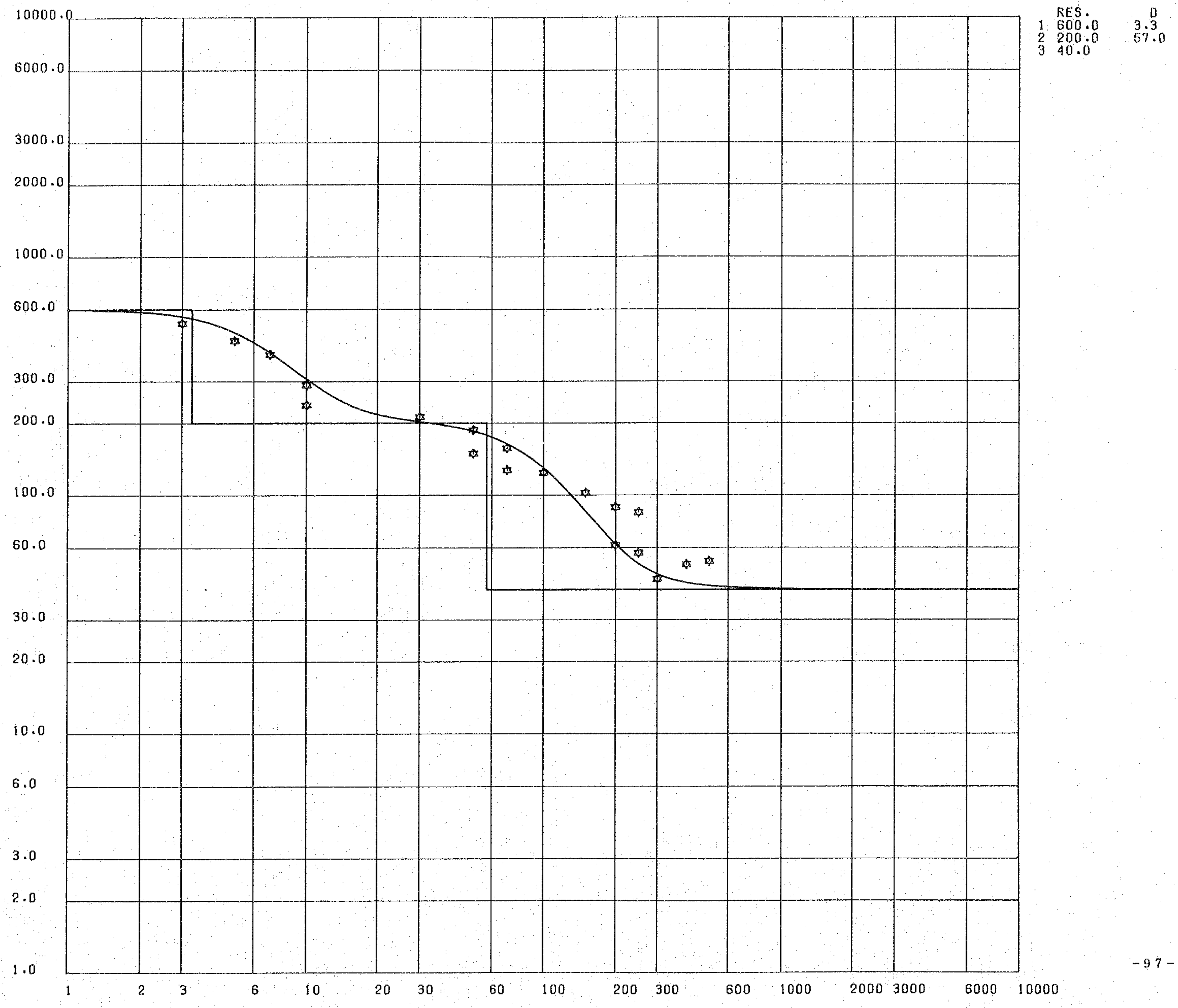

V. ROCK ALTERATION SURVEY

[illegible]

CHAPTER 1 INTRODUCTION

The present status of geothermal exploration in Kenya has been reported by Noble and Ojiambo (1975). According to them, geological, geophysical and geochemical surveys were carried out in three of the most promissing area, that is Lake Bogoria, Eburru and Olkaria by the Unite Nations Development Program (UNDP). As the result, Olkaria, about 100 km northeast of Nairobi, was given first priority for geothermal exploration in Kenya. Thus a first geothermal power plant (15 MWe) in Africa was completed by 1981 and another (15 MWe) unit was also inaugurated in 1982 by East African Power and Lighting Company Limited (EAP & L).

On the other hand, a geothermal exploration project was started in 1979 at Eburru, 30 km north of Olkaria, as a joint project between the Governments of Kenya and Japan.

The purpose of the present report is to describe the rock alteration study carried out between November, 1980 and February, 1981, as one of geological survey in the Eburru geothermal field.

CHAPTER 2 GEOLOGICAL SETTING

The Rift Valley was formed by two times of major faulting in late Miocene and late Pliocene. The geothermal systems of the Rift Valley are located within Miocene to Recent volcanic rocks covering unconformably the Precambrian basement rocks.

There are many active volcanoes such as Menengai, Ol Doinyo Eburru, Longonot and Ol Doinyo Nyukie (Suswa) in the Rift Valley. The Eburru geothermal field in question is situated on the active volcano of Ol Doinyo Eburru which is classified into a compound volcano. According to the "Catalogue of the active volcanoes and solfatras of the world (1957)", the volcano of Ol Doinyo Eburru consists of an E–W stretching volcanic body, and no eruptions have been recorded since the first explorers reached the interior of East Africa.

The geology of this area has been reported by Thompson and Dodson (1963). Naylor (1971, 1972 unpub.) also reported in detail the geology of Eburru as well as those of Lake Bogoria and Olkaria for geothermal exploration project carried out by the UNDP. Satoh (1981) investigated the geology of the Eburru geothermal field for the present project and geology will be described in detail in II. According to Satoh, outline of the geology is as follows:

The Ol Doinyo Opur Pumice – Fall Deposits (more than 20 m in thickness) are widely distributed in the Eburru geothermal field overlying the Formations of Welded Tuff and Phonolite & Comendite of Pleistocene in age. It is intruded by numerous dykes of banded obsidian extending N – S direction, and it is covered by the Obsidian Lava Flow Formation in the western area. Some obsidian lava domes and volcanic ash cones are found around Cedar Hill which is composed of obsidian lava dome (1.3 km in width). The Older Badland Basalt Formation consisting of olivine basalt is distributed near Eburru Station. The Younger Pumice-Fall Deposits covered the surface in this field.

CHAPTER 3 OUTLINE OF GEOTHERMAL ACTIVITIES

There are many thermal manifestations such as fumaroles and hot grounds with alteration halo in the Eburru Geothermal Prospect (Pl. V–1). They are found around explosion craters of the active volcano of Ol Doinyo Eburru. They are also found along the faults extending N – S direction in the northern foot area of the volcano. The IR survey conducted by the UNDP shows about 170 thermal patches of ground. It cannot, however, detect any thermal manifestations in the south, west and east areas of the volcano. We cannot also find any hot-springs on the surface because of the lack of water.

The heat discharged area is about 45 km^2, and the natural heat discharge is estimated to be 31,000 Kcal/sec which is equivalent to 130MWt by the UNDP report.

Natural steam is utilized by the local people to get condensed water and to dry pyrethrum flowers.

CHAPTER 4 SPECIMENS AND METHOD OF STUDY

A field work was carried out for mapping of alteration zone, sampling of altered rocks and check of the ground temperature. About 160 rock samples were collected from the Eburru geothermal field and samples for X-ray analysis are prepared as follows:

The rock sample is crushed into fine powder less than 60 mesh in a stainless mortar and the fine powder is ground in an agate mortar for five minutes. About 70 samples* thus obtained were analyzed by means of an X-ray diffractometer "MINIFLEX" of the Ministry of Energy, Kenya.

Experimental conditions are as follows:

Radiation Cuk (λ = 1.5418Å), voltage 30 KV (fixed) current 10 mA (fixed), time constant 1 sec., full scale 500 or 1000 cps, scanning speed 2°/min., chart speed 20 mm/min.

* One hundred samples were separately examined by an X-ray deffractometer in Japan for detailed identification of alteration product. The result is given in Appendix 1.

CHAPTER 5 ALTERATION PRODUCTS

Although further examination are actually required to determine the mineralogical properties, alteration products confirmed by X-ray powder diffraction method are as follows :

Clay minerals : Montmorillonite, kaolinite, halloysite, allophane

Silica Minerals : Quartz, α-cristobalite, β-cristobalite

Carbonate Mineral : Calcite

Zeolite : Clinoptilolite or heulandite

The rock alteration in the Eburru geothermal field can be divided into five zones and one distribution area on the basis of mineral association.

Zone I : Kaolinite (well-crystallized) – β-cristobalite – quartz

Zone II : Kaolinite (well-crystallized) – quartz

Zone III : Kaolinite (well- and/or poor-crystallized) – quartz

Zone IV : Halloysite and/or allophane

Zone V : Montmorillonite

Distribution area of sinter (calcite).

Sulfide and sulfate minerals such as pyrite, alunite and gypsum were not at all recognized so far in this field.

CHAPTER 6 ZONAL DISTRIBUTION OF ALTERATION ZONES

Zonal distribution map of alteration zones is shown in Pl. V–2.

Zone I is characterized by the presence of well-crystallized kaolinite, β-cristobalite and quartz, and it indicates the highest grade of alteration in this field because of the presence of β-cristobalite.* High temperature minerals such as diaspore, pyrophyllite and dickite could not be, however, detected in this zone. Zone I occurs quite locally in the Eburru Crater area.

Zone II is characterized by the presence of well-crystallized kaolinite and quartz, and it is distinguished from Zone I by the absence of β-cristobalite. Zone II is distributed in the Eburru Crater area surrounding Zone I. Silicified rock and quartz vein are locally found in Zones I and II, and several kaolin deposits are in operation in both zones.

Zone III is characterized by the presence of well-crystallized and/or poor-crystallized kaolinites and quartz. It extends from west to east in the Eburru Crater area surrounding Zone II.

Zone IV is characterized by the formation of halloysite and/or allophane. It is distinguished from Zone III by the disappearance of kaolinite. Zone IV is found in the northern foot of the Eburru Crater area extending N–S direction along the faults whereas Zones II and III extends in W–E direction which is nearly parallel to the alignment of explosion craters in the Eburru Crater area.

Zone V is characterized by the formation of montmorillonite. This zone occurs in the northern area of Zone IV and it seems to disappear at the northeast of Eburru Station in which the thermal patches of ground detected by IR survey also disappear.

Distribution area of sinter (calcite) is found in Zone V near Eburru Station. Sinter mainly occurs filling cavities of porous scoria of the Older Badland Formation.

As shown in Pl. V–2, these alteration zones give a zonal arrangement from center (Zone I) to margin (Zone V) in the northern area of Eburru Crater. The distribution of alteration zones is, however, restricted to the southern area of Eburru Crater.

* α-cristobalite is experimentally transformed into β-cristobalite by heating between 220°C and 280°C.
α-cristobalite is also transformed into quartz under the condition lower than 100°C in the geothermal field.

CHAPTER 7 DISCUSSION

As mentioned above, the distribution of alteration zones shows a zonal arrangement from Zone I (center) to Zone V (margin). Zones I and II in the Eburru Crater area give intense rock alteration because of the predominant presence of well-crystallized kaolinite. Occurrence of β-cristobalite suggests that Zone I was produced under the high temperature condition between 200°C and 300°C. Although Zones I and II show an acid-leached zone, such superficial leached halo can be caused by not only acidic solution but also vapor. In this case, it is considered that both zones would be produced by vapor rather than acidic solution, because any hot-springs cannot be observed on the surface in this area.

On the other hand, Zone V in the margin area is characterized by the presence of low temperature products such as montmorillonite and α-cristobalite. Zeolite and calcareous sinter (calcite) are also found in this zone. In general, these alteration products are formed by low temperature alkaline water.

As stated already, Zones I, II and III are distributed in the Eburru Crater area, which is nearly located at the center of the active volcano of Ol Doinyo Eburru with E–W stretching volcanic body. On the contrary, Zones IV and V are distributed along or parallel to the faults extending N–S direction in the northern foot of the Eburru Crater area.

Judging from the above facts, although the scientific information is more limited, the geothermal system in this field can be explained as follows:

In the light of the distribution of alteration zones, it is suggested that the center of heat source such as magma reservoir is in the vicinity beneath the Eburru Crater area. This hypothesis is also supported by the distribution of explosion craters of the Ol Doinyo Eburru and the gas analysis data carried out by the UNDP which show low air contamination in this area.

The deep water beneath the Eburru Crater area becomes a brine by dissolved substances under the conductive heat from the magma reservoir. With time, channels of inflowing water are narrowed or diminished by precipitation of alteration products. Such under self-sealing condition, a vapor dominated system containing liquid water and vapor coexisting is formed above the brine. Vapor from brine is superheated above the water table. The superheated vapor and other gases (CO_2, CH_4 and H_2S) rise in the outlet channels with decreasing temperature and pressure. Finally they discharge at the surface from fumaroles. Altered zone is formed by reaction of vapor and/or water derived from condensing steam rich in CO_2 with rock silicates. Thus the leached zones such as Zones I and II were formed in the Eburru Crater area.

On the other hand, the hot brine rising in the Eburru Crater area gradually flows down to the Eburru Station area. It flows from south to north along the water table with decreasing temperature, and steam from the hot brine issues along the faults extending N–S direction. Finally the hot brine would approach nearest to the surface in the Eburru Station area, though any hot-springs cannot be found. Thus Zone V, which is characterized by the presence of calcite and zeolite in association with montmorillonite, was formed in the Eburru Station area. Zone V is characteristic of alteration by hot-water geothermal system.

Although available data are scanty, it is concluded that the Eburru geothermal field has a vapor-dominated geothermal system after White et al. (1971). However, as there are no information on the geology of reservoir in the Eburru geothermal field, additional geological, geophysical and geochemical surveys including drilling are actually required in the future before exploitation.

Supplement for Rock Alteration Survey in the Interim Report II (1981)

We reexamined in detail the X-ray diffraction data given in Appendix 1 of the Interim Report II (1981). As the result, we identified the following new alteration products in the Eburru geothermal area; sulfate minerals such as alunite and alunogen, and kaolin/montmorillonite mixed-layer mineral. So we would present the revised alteration zoning and distribution areas of alteration products as follows:

Alteration zoning in 1982		Alteration zoning in 1981
Zone I :	Alunite Zone with alunogen, kaolinite (well-crystallized), β-cristobalite and quartz	Zone I
Zone IIa :	Kaolinite Zone (well-crystallized) with boemite, β-cristobalite and quartz	Zone II
Zone IIb :	Kaolinite Zone (poor-crystallized) with α-cristobalite and quartz	Zone III
Zone III :	Montmorillonite Zone with kaolin/montmorillonite mixed-layer mineral and halloysite	Zone V
Distribution area of calcareous sinter		Distribution area of sinter (calcite)
Distribution area of β-cristobalite		Zone I
Distribution area of allophane		Zone IV

A zonal distribution map of alteration zones revised in this time is shown in Pl. V–2. The distribution of Zones I (Alunite Zone), II (Kaolinite Zone) and III (Montmorillonite Zone) clearly show zonal arrangement in the Eburru Crater area. Such zonal arrangement of alteration can be observed in many typical geothermal areas of Japan.

Chemically, alunite which is the highest grade zone in the Eburru area is formed by interaction between rock and condensed water containing sulfate ions derived from dissolution of volcanic gases (H_2S and SO_2) in H_2O. It is clear that such gases are coming up through the vents of active volcano, Ol Doinyo Eburru.

So we present a genetic model of Eburru geothermal area depicted in Fig. 5 on the basis of rock alteration survey. Fig. 5 shows the cross-section through the Eburru Crater, from the Lake Naivasha to the Lake Elementeita. As the water level of Lake Naivasha is the highest in the Rift Valley, groundwater which infltrate through the Lake Naivasha may flow along the slope of water level from south to north, and it passes through the center of active volcano where the ground water is superheated.

Superheated vapor including gases is discharged from fumarloes areas developing along the faults extending N-S direction. Calcareous sinter is precipitated from hot water near the surface at Eburru Station area, and finally hot water issues on the southern shore of the Lake Elementeita.

REFERENCES

Noble, J.W. and Ojiambo, S.B. (1975) Geothermal exploration in Kenya. Proc. 2nd UN symp. on the development and use of geothermal resources. Vol. I, 189–204.

Thompson, A.O. and Dodson, R.G. (1963) Geology of the Naivasha area. Geological Survey of Kenya.

White, D.E., Muffler, L.J.P. and Truesdell, A.H. (1971) Vapor-dominated hydrothermal systems compared with hot-water systems. Econ. Geol., Vol. 66, 75–97.

Table V–1 X-ray Diffraction Data for Altered Rocks

No.	Sample No.	Lithology \ Minerals	Silica minerals				Altered minerals							Sulfates & carbonates				Others				Primary minerals						
			α–Cristobalite	β–Cristobalite	α–Quartz		Allophane (amorphous)	Montmorillonite	Montmorillonite/Kaolinite	Kaolinite	Boemite	Clinopilolite		Alunite	Alunogen	Calcite		Magnetite	Hematite	Marcasite	Sinhalite	Feldspar	Hornblende	Aenigmatite	Augite	Acmite	Mica	
97	E–149	altered silicified rock (white)		◎	△					○																		
98	E–150	porous argillized rock (white)		◎	△					○																		
99	E–152	porous silicified rock (white)	◎	△	○					◎																		
100	E–153	clay (white)								◎																		
101	E–33				○				◎	△												◎	○			△		
102	E–42				△				◎	○												△						
103	E–55				○																	◎	◎					
104	E–73								◎	○								•										
105	E–98				◎				•													○						
106	E–106							○	○	○																		
107	E–112				○					◎																		
108	E–128			△	•		•			•									△			△						
109	E–148				○					◎				△														
110	E–152		◎	△	○					◎																		

Symbols : ◎ abundunt, ○ common, △ a little, rare, ? uncertain

Table IV-2-(1) Resistivity Field Data at E Line, Point 108

AB/2	MN/2	K	I (Amp)	V (mV)	R (Ω m)
3	1	12.6	0.20	2,520	159
5	1	37.7	0.20	943	178
7	1	75.4	0.20	520	196
10	1	156	0.20	298	232
10	3	47.6	0.20	893	213
15	3	113	0.20	407	230
15	1	352	0.20	138	243
20	3	205	0.20	213	218
30	3	467	0.20	78.3	183
50	3	1,300	0.20	19.8	129
50	10	377	0.20	65.7	124
70	10	754	0.20	31.3	118
70	3	2,560	0.20	9.73	125
100	10	1,560	0.20	11.8	92.0
150	10	3,520	0.20	3.17	55.8
200	10	6,270	0.20	1.53	48.0
200	50	1,180	0.20	8.90	52.5
250	50	1,880	0.16	3.60	42.3
250	10	9,800	0.16	0.663	40.6
300	50	2,750	0.16	1.79	30.8
400	50	4,950	0.20	1.13	28.0
500	50	7,780	0.30	1.03	26.7
500	100	3,770			
700	100	7,540			
700	50	15,300			
1,000	100	15,600			
1,200	100	22,500			
1,500	100	35,200			

Table IV-2-(2) Resistivity Field Data at E Line, Point 113

AB/2	MN/2	K	I (Amp)	V (mV)	R (Ω m)
3	1	12.6	0.10	2,500	315
5	1	37.7	0.10	1,860	701
7	1	75.4	0.10	860	648
10	1	156	0.14	600	669
10	3	47.6	0.14	1,680	571
15	3	113	0.20	1,060	599
15	1	352	0.20	392	690
20	3	205	0.20	523	536
30	3	467	0.20	168	392
50	3	1,300	0.20	47.3	307
50	10	377	0.20	141	266
70	10	754	0.20	74.3	280
70	3	2,560	0.20	19.3	247
100	10	1,560	0.20	72.7	227
150	10	3,520	0.20	7.50	52.8
200	10	6,270	0.50	5.37	67.3
200	50	1,180	0.50	20.9	49.3
250	50	1,880	0.50	12.1	45.5
250	10	9,800	0.50	3.38	66.2
300	50	2,750	0.45	7.07	43.2
400	50	4,950	0.30	2.67	44.1
500	50	7,780	0.30	1.69	43.8
500	100	3,770			
700	100	7,540			
700	50	15,300	0.50	1.25	38.3
1,000	100	15,600			
1,200	100	22,500			
1,500	100	35,200			

Table IV-2-(3) Resistivity Field Data at E Line, Point 118

AB/2	MN/2	K	I (Amp)	V (mV)	R (Ω m)
3	1	12.6	0.20	1,490	93.9
5	1	37.7	0.20	470	88.6
7	1	75.4	0.20	270	102
10	1	156	0.20	153	119
10	3	47.6	0.20	447	106
15	3	113	0.20	267	151
15	1	352	0.20	94.3	166
20	3	205	0.20	176	180
30	3	467	0.20	83.7	195
50	3	1,300	0.30	38.5	167
50	10	377	0.30	138	173
70	10	754	0.30	44.0	111
70	3	2,560	0.30	12.6	108
100	10	1,560	0.30	5.50	28.6
150	10	3,520	0.30	2.95	34.6
200	10	6,270	0.20	1.03	32.3
200	50	1,180	0.20	6.53	38.5
250	50	1,880	0.20	3.47	32.6
250	10	9,800	0.20	0.59	28.9
300	50	2,750	0.20	2.35	32.3
400	50	4,950	0.20	1.38	34.2
500	50	7,780	0.20	0.85	33.1
500	100	3,770	0.20	1.90	35.8
700	100	7,540	0.30	1.28	32.2
700	50	15,300	0.30	0.577	29.4
1,000	100	15,600	0.30	0.407	21.2
1,200	100	22,500			
1,500	100	35,200			

Table IV-2-(4) Resistivity Field Data at E Line, Point 123

AB/2	MN/2	K	I (Amp)	V (mV)	R (Ω m)
3	1	12.6	0.20	2,570	162
5	1	37.7	0.20	2,250	424
7	1	75.4	0.20	1,420	535
10	1	156	0.20	767	598
10	3	47.6	0.20	2,420	576
15	3	113	0.20	1,330	751
15	1	352	0.20	440	774
20	3	205	0.20	793	813
30	3	467	0.20	350	817
50	3	1,300	0.20	113	735
50	10	377	0.20	400	754
70	10	754	0.30	176	442
70	3	2,560	0.30	49.0	418
100	10	1,560	0.20	34.2	267
150	10	3,520	0.30	17.6	207
200	10	6,270	0.30	9.32	195
200	50	1,180	0.30	44.6	175
250	50	1,880	0.30	20.4	128
250	10	9,800	0.30	4.35	142
300	50	2,750	0.21	6.93	90.8
400	50	4,950	0.21	2.01	47.4
500	50	7,780	0.20	0.96	37.3
500	100	3,770			
700	100	7,540			
700	50	15,300	0.20	0.393	30.1
1,000	100	15,600			
1,200	100	22,500			
1,500	100	35,200			

Table IV-2-(5) Resistivity Field Data at E Line, Point 128

AB/2	MN/2	K	I (Amp)	V (mV)	R (Ω m)
3	1	12.6	0.30	6,100	256
5	1	37.7	0.18	1,030	216
7	1	75.4	0.27	740	207
10	1	156	0.15	220	229
10	3	47.6	0.15	630	200
15	3	113	0.15	290	218
15	1	352	0.15	103	242
20	3	205	0.15	182	248
30	3	467	0.30	163	253
50	3	1,300	0.18	32.5	235
50	10	377	0.18	117	245
70	10	754	0.24	84.0	264
70	3	2,560	0.24	23.5	251
100	10	1,560	0.24	42.2	274
150	10	3,520	0.24	16.7	245
200	10	6,270	0.24	6.70	175
200	50	1,180	0.24	47.5	234
250	50	1,880	0.24	20.6	161
250	10	9,800	0.24	2.97	121
300	50	2,750	0.12	3.95	90.5
400	50	4,950	0.30	2.50	41.3
500	50	7,780	0.20	0.967	37.6
500	100	3,770			
700	100	7,540			
700	50	15,300			
1,000	100	15,600			
1,200	100	22,500			
1,500	100	35,200			

Table IV-2-(6) Resistivity Field Data at H Line, Point 94

AB/2	MN/2	K	I (Amp)	V (mV)	R (Ω m)
3	1	12.6	0.10	1,233	155
5	1	37.7	0.08	233	110
7	1	75.4	0.16	253	119
10	1	156	0.20	159	124
10	3	47.6	0.20	473	113
15	3	113	0.08	80.7	114
15	1	352	0.08	27.7	122
20	3	205	0.14	80.0	117
30	3	467	0.20	51.7	121
50	3	1,300	0.12	10.8	117
50	10	377	0.12	38.8	122
70	10	754	0.08	10.8	102
70	3	2,560	0.08	3.05	97.6
100	10	1,560	0.08	3.53	68.8
150	10	3,520	0.08	1.23	54.1
200	10	6,270	0.10	0.697	43.7
200	50	1,180	0.10	4.73	55.8
250	50	1,880	0.30	7.13	44.7
250	10	9,800	0.30	1.08	35.3
300	50	2,750	0.20	2.57	35.3
400	50	4,950	0.14	0.883	31.2
500	50	7,780	0.30	1.03	26.7
500	100	3,770			
700	100	7,540			
700	50	15,300			
1,000	100	15,600			
1,200	100	22,500			
1,500	100	35,200			

Table IV-2-(7) Resistivity Field Data at H Line, Point 99

AB/2	MN/2	K	I (Amp)	V (mV)	R (Ω m)
3	1	12.6	0.10	2,330	294
5	1	37.7	0.08	983	463
7	1	75.4	0.10	470	354
10	1	156	0.16	387	377
10	3	47.6	0.16	1,020	303
15	3	113	0.16	440	311
15	1	352	0.16	178	392
20	3	205	0.10	144	295
30	3	467	0.14	66.3	221
50	3	1,300	0.14	22.8	212
50	10	377	0.14	57.3	154
70	10	754	0.20	34.5	130
70	3	2,560	0.20	11.9	152
100	10	1,560	0.10	6.83	107
150	10	3,520	0.10	2.62	92.2
200	10	6,270	0.16	1.72	67.4
200	50	1,180	0.16	12.5	92.2
250	50	1,880	0.20	7.10	66.7
250	10	9,800	0.20	10.2	50.0
300	50	2,750	0.08	1.46	50.2
400	50	4,950	0.08	0.70	43.3
500	50	7,780	0.30	1.44	37.3
500	100	3,770			
700	100	7,540			
700	50	15,300	0.80	1.69	32.3
1,000	100	15,600			
1,200	100	22,500			
1,500	100	35,200			

Table IV-2-(8) Resistivity Field Data at H Line, Point 104

AB/2	MN/2	K	I (Amp)	V (mV)	R (Ω m)
3	1	12.6	0.08	1,780	280
5	1	37.7	0.30	1,630	205
7	1	75.4	0.30	757	190
10	1	156	0.10	112	175
10	3	47.6	0.10	307	146
15	3	113	0.20	219	124
15	1	352	0.20	83.7	147
20	3	205	0.20	141	145
30	3	467	0.50	134	125
50	3	1,300	0.30	20.7	89.7
50	10	377	0.30	69.3	87.1
70	10	754	0.50	49.3	74.3
70	3	2,560	0.50	15.2	77.8
100	10	1,560	0.20	7.93	61.9
150	10	3,520	0.16	2.33	51.3
200	10	6,270	0.08	0.64	50.2
200	50	1,180	0.08	3.37	49.7
250	50	1,880	0.20	3.47	32.6
250	10	9,800	0.20	0.65	31.9
300	50	2,750	0.20	1.88	25.9
400	50	4,950	0.20	0.80	19.8
500	50	7,780	0.20	0.707	27.5
500	100	3,770			
700	100	7,540			
700	50	15,300	0.10	0.183	28.0
1,000	100	15,600			
1,200	100	22,500			
1,500	100	35,200			
1,000	50	31,300	0.64	0.467	22.8

Table IV-2-(9) Resistivity Field Data at H Line, Point 109

AB/2	MN/2	K	I (Amp)	V (mV)	R (Ω m)
3	1	12.6	0.20	2,530	159
5	1	37.7	0.20	1,230	232
7	1	75.4	0.20	1,030	388
10	1	156	0.20	570	445
10	3	47.6	0.20	1,820	433
15	3	113	0.20	787	445
15	1	352	0.20	247	435
20	3	205	0.20	493	505
30	3	467	0.12	170	662
50	3	1,300	0.12	62.7	679
50	10	377	0.12	273	858
70	10	754	0.12	80.0	503
70	3	2,560	0.12	16.8	358
100	10	1,560	0.30	71.7	373
150	10	3,520	0.30	10.0	117
200	10	6,270	0.30	4.07	85.1
200	50	1,180	0.30	15.0	59.0
250	50	1,880	1.00	29.0	54.5
250	10	9,800			
300	50	2,750	0.30	5.97	54.7
400	50	4,950	0.20	1.70	42.1
500	50	7,780	0.30	1.40	36.3
500	100	3,770	0.30	2.58	32.4
700	100	7,540	0.20	0.747	28.2
700	50	15,300	0.20	0.443	33.9
1,000	100	15,600	0.35	0.623	27.8
1,200	100	22,500	0.64	0.727	25.6
1,500	100	35,200			

Table IV-2-(10) Resistivity Field Data at H Line, Point 114

AB/2	MN/2	K	I (Amp)	V (mV)	R (Ω m)
3	1	12.6	0.20	237	14.9
5	1	37.7	0.20	100	18.9
7	1	75.4	0.20	36.7	13.8
10	1	156	0.16	28.2	27.5
10	3	47.6	0.16	87.3	26.0
15	3	113	0.16	52.3	36.9
15	1	352	0.16	17.2	37.8
20	3	205	0.16	35.2	45.1
30	3	467	0.16	21.2	61.9
50	3	1,300	0.16	13.8	112
50	10	377	0.16	44.0	104
70	10	754	0.16	26.3	124
70	3	2,560	0.16	8.23	132
100	10	1,560	0.16	10.8	105
150	10	3,520	0.16	3.12	68.6
200	10	6,270	0.16	1.11	43.5
200	50	1,180	0.16	5.37	39.6
250	50	1,880	0.12	2.37	37.1
250	10	9,800	0.12	0.51	41.7
300	50	2,750	0.12	1.02	23.4
400	50	4,950	0.20	0.767	19.0
500	50	7,780	0.20	0.473	18.4
500	100	3,770	0.20	1.61	30.3
700	100	7,540	0.24	0.847	26.6
700	50	15,300	0.24	0.263	16.8
1,000	100	15,600	0.24	0.390	25.4
1,200	100	22,500	0.18	0.187	23.4
1,500	100	35,200	0.12	0.080	23.5

Table IV-2-(11) Resistivity Field Data at H Line, Point 120

AB/2	MN/2	K	I (Amp)	V (mV)	R (Ω m)
3	1	12.6	0.12	2,400	252
5	1	37.7	0.12	1,530	481
7	1	75.4	0.12	917	576
10	1	156	0.12	570	741
10	3	47.6	0.12	1,560	619
15	3	113	0.12	620	584
15	1	352	0.12	232	681
20	3	205	0.12	468	800
30	3	467	0.12	225	876
50	3	1,300	0.08	76.3	1,240
50	10	377	0.08	173	815
70	10	754	0.08	96.7	911
70	3	2,560	0.08	43.2	1,382
100	10	1,560	0.08	47.7	930
150	10	3,520	0.18	29.3	573
200	10	6,270	0.18	6.67	232
200	50	1,180	0.18	26.5	174
250	50	1,880	0.18	4.97	51.9
250	10	9,800	0.18	1.23	67.0
300	50	2,750	0.80	12.4	42.6
400	50	4,950	0.80	3.03	18.7
500	50	7,780	0.56	1.88	26.1
500	100	3,770	0.56	4.30	28.9
700	100	7,540	0.56	1.73	23.3
700	50	15,300	0.56	0.80	21.9
1,000	100	15,600	0.30	0.437	22.7
1,200	100	22,500	0.12	0.119	22.3
1,500	100	35,200	0.24	0.153	22.4

Table IV-2-(12) Resistivity Field Data at H Line, Point 124

AB/2	MN/2	K	I (Amp)	V (mV)	R (Ω m)
3	1	12.6	0.20	9,000	567
5	1	37.7	0.20	3,360	633
7	1	75.4	0.20	1,674	631
10	1	156	0.20	828	646
10	3	47.6	0.20	2,100	500
15	3	113	0.20	925	523
15	1	352	0.20	380	669
20	3	205	0.20	520	533
30	3	467	0.20	273	637
50	3	1,300	0.20	91.7	596
50	10	377	0.20	327	616
70	10	754	0.20	164	618
70	3	2,560	0.20	46.7	598
100	10	1,560	0.20	75.0	585
150	10	3,520	0.20	16.5	290
200	10	6,270	0.20	3.80	119
200	50	1,180	0.20	20.2	119
250	50	1,880	0.20	6.57	61.8
250	10	9,800	0.20	0.65	31.9
300	50	2,750	0.20	3.72	51.2
400	50	4,950	0.30	1.76	29.0
500	50	7,780	2.00	6.10	23.7
500	100	3,770	2.00	12.4	23.4
700	100	7,540	1.20	3.18	20.0
700	50	15,300	1.20	1.61	20.5
1,000	100	15,600	0.20	0.247	19.3
1,200	100	22,500	0.50	0.42	18.9
1,500	100	35,200	0.50	0.28	19.7

Table IV-2-(13) Resistivity Field Data at H Line, Point 129

AB/2	MN/2	K	I (Amp)	V (mV)	R (Ω m)
3	1	12.6	0.16	1,040	81.9
5	1	37.7	0.16	407	95.9
7	1	75.4	0.16	235	111
10	1	156	0.16	142	138
10	3	47.6	0.16	437	130
15	3	113	0.16	257	182
15	1	352	0.16	88.0	194
20	3	205	0.16	190	243
30	3	467	0.16	113	330
50	3	1,300	0.20	72.6	472
50	10	377	0.20	222	418
70	10	754	0.20	108	407
70	3	2,560	0.20	32.5	416
100	10	1,560	0.20	44.7	349
150	10	3,520	0.20	7.40	130
200	10	6,270	0.20	2.65	83.1
200	50	1,180	0.20	12.9	76.1
250	50	1,880	0.20	7.97	74.9
250	10	9,800	0.20	1.13	55.4
300	50	2,750	0.20	3.57	49.1
400	50	4,950	0.30	1.71	28.2
500	50	7,780	0.50	1.54	24.0
500	100	3,770	0.50	3.90	29.4
700	100	7,540	0.30	1.01	25.4
700	50	15,300	0.30	0.413	21.1
1,000	100	15,600	0.50	0.713	22.2
1,200	100	22,500	0.50	0.553	24.9
1,500	100	35,200			

Table IV-2-(14) Resistivity Field Data at H Line, Point 134

AB/2	MN/2	K	I (Amp)	V (mV)	R (Ω – m)
3	1	12.6	0.50	2,600	65.5
5	1	37.7	0.50	1,710	129
7	1	75.4	0.50	1,040	157
10	1	156	0.50	607	189
10	3	47.6	0.50	1,690	161
15	3	113	0.50	975	220
15	1	352	0.50	358	252
20	3	205	0.50	690	283
30	3	467	0.50	422	394
50	3	1,300	0.50	197	512
50	10	377	0.50	630	475
70	10	754	0.80	607	572
70	3	2,560	0.80	191	611
100	10	1,560	1.00	383	597
150	10	3,520	0.80	63.7	280
200	10	6,270	0.80	11.8	92.5
200	50	1,180	0.80	70.3	104
250	50	1,880	0.80	33.7	79.2
250	10	9,800	0.80	8.53	104
300	50	2,750	0.50	23.3	128
400	50	4,950	0.80	7.03	43.5
500	50	7,780	0.20	0.91	35.4
500	100	3,770	0.20	1.63	30.7
700	100	7,540	0.50	1.75	26.4
700	50	15,300	0.50	0.992	30.4
1,000	100	15,600	1.00	1.69	26.4
1,200	100	22,500			
1,500	100	35,200			

Table IV-2-(15) Resistivity Field Data at H Line, Point 139

AB/2	MN/2	K	I (Amp)	V (mV)	R (Ω m)
3	1	12.6	0.30	2,600	109
5	1	37.7	0.30	1,430	180
7	1	75.4	0.30	753	189
10	1	156	0.30	317	165
10	3	47.6	0.30	970	154
15	3	113	0.30	332	125
15	1	352	0.30	113	133
20	3	205	0.30	144	98.4
30	3	467	0.30	55.0	85.6
50	3	1,300	0.30	24.7	107
50	10	377	0.30	86.7	109
70	10	754	0.30	50.3	126
70	3	2,560	0.30	14.5	124
100	10	1,560	0.30	24.3	126
150	10	3,520	0.30	9.40	110
200	10	6,270	0.30	5.57	116
200	50	1,180	0.30	22.8	89.7
250	50	1,880	0.20	7.03	66.1
250	10	9,800	0.20	1.75	85.8
300	50	2,750	0.30	5.70	52.3
400	50	4,950	0.30	1.64	27.1
500	50	7,780	0.80	2.21	21.5
500	100	3,770			
700	100	7,540	0.80	1.12	10.6
700	50	15,300			
1,000	100	15,600			
1,200	100	22,500			
1,500	100	35,200			

Table IV-2-(16) Resistivity Field Data at K Line, Point 101

AB/2	MN/2	K	I (Amp)	V (mV)	R (Ω m)
3	1	12.6	0.14	6,670	600
5	1	37.7	0.14	2,820	759
7	1	75.4	0.10	777	586
10	1	156	0.06	182	473
10	3	47.6	0.06	322	255
15	3	113	0.08	166	234
15	1	352	0.08	70.7	311
20	3	205			
30	3	467			
50	3	1,300			
50	10	377	0.30	74.3	93.4
70	10	754	0.30	26.7	67.1
70	3	2,560			
100	10	1,560	0.20	6.13	47.8
150	10	3,520	0.30	2.98	35.0
200	10	6,270	0.14	0.68	30.5
200	50	1,180	0.14	5.37	45.3
250	50	1,880	0.10	2.90	54.5
250	10	9,800	0.10	0.333	32.6
300	50	2,750	0.05	0.787	43.3
400	50	4,950	0.30	1.59	26.2
500	50	7,780	0.50	1.64	25.5
500	100	3,770			
700	100	7,540			
700	50	15,300			
20	1	627	0.06	19.3	202
30	1	1,410	0.10	8.3	117
50	1	3,930	0.30	7.33	96.0
70	1	7,700	0.30	3.23	82.9

Table IV-2-(17) Resistivity Field Data at K Line, Point 106

AB/2	MN/2	K	I (Amp)	V (mV)	R (Ω m)
3	1	12.6	0.20	6,270	395
5	1	37.7	0.20	2,920	550
7	1	75.4	0.20	1,660	626
10	1	156	0.16	640	624
10	3	47.6	0.16	2,080	619
15	3	113	0.16	727	513
15	1	352	0.16	235	517
20	3	205	0.16	392	502
30	3	467	0.12	91.7	357
50	3	1,300	0.06	9.03	196
50	10	377	0.06	29.0	182
70	10	754	0.10	26.8	202
70	3	2,560	0.10	8.97	230
100	10	1,560	0.20	14.1	110
150	10	3,520	0.14	3.32	83.5
200	10	6,270	0.30	2.85	59.6
200	50	1,180	0.30	17.7	69.6
250	50	1,880	0.30	8.57	53.7
250	10	9,800	0.30	1.38	45.1
300	50	2,750	0.20	3.25	44.7
400	50	4,950	0.50	3.45	34.2
500	50	7,780	0.16	0.50	24.3
500	100	3,770			
700	100	7,540			
700	50	15,300	0.40	0.857	32.8
1,000	100	15,600			
1,200	100	22,500			
1,500	100	35,200			

Table IV-2-(18) Resistivity Field Data at K Line, Point 111

AB/2	MN/2	K	I (Amp)	V (mV)	R (Ω m)
3	1	12.6	0.06	3,020	634
5	1	37.7	0.10	1,080	407
7	1	75.4	0.08	387	365
10	1	156	0.10	192	300
10	3	47.6	0.10	530	252
15	3	113	0.20	437	247
15	1	352	0.20	177	312
20	3	205	0.20	237	243
30	3	467	0.04	21.7	253
50	3	1,300	0.20	38.2	248
50	10	377	0.30	180	226
70	10	754	0.15	41.8	210
70	3	2,560	0.15	13.5	230
100	10	1,560	0.15	16.8	175
150	10	3,520	0.10	3.50	123
200	10	6,270	0.08	1.00	78.4
200	50	1,180	0.08	4.75	70.1
250	50	1,880	0.20	5.63	52.9
250	10	9,800	0.20	1.20	58.8
300	50	2,750	0.10	1.73	47.6
400	50	4,950	0.10	0.89	44.1
500	50	7,780	0.30	1.55	40.2
500	100	3,770			
700	100	7,540			
700	50	15,300	0.30	0.473	24.1
1,000	100	15,600			
1,200	100	22,500			
1,500	100	35,200			

Table IV-2-(19) Resistivity Field Data at K Line, Point 116

AB/2	MN/2	K	I (Amp)	V (mV)	R (Ω m)
3	1	12.6	0.20	6,930	437
5	1	37.7	0.06	700	440
7	1	75.4	0.06	333	418
10	1	156	0.10	413	644
10	3	47.6	0.10	1,360	647
15	3	113	0.10	667	754
15	1	352	0.10	208	732
20	3	205	0.20	810	830
30	3	467	0.12	205	798
50	3	1,300	0.06	18.8	407
50	10	377	0.06	48.3	303
70	10	754	0.06	20.6	259
70	3	2,560	0.06	8.10	346
100	10	1,560	0.20	16.8	131
150	10	3,520	0.10	3.25	114
200	10	6,270	0.20	4.00	125
200	50	1,180	0.20	28.3	167
250	50	1,880	0.20	16.4	154
250	10	9,800	0.20	2.43	119
300	50	2,750	0.20	11.7	161
400	50	4,950	0.16	1.98	61.3
500	50	7,780	0.30	1.13	29.3
500	100	3,770			
700	100	7,540			
700	50	15,300	0.30	0.313	16.0
1,000	100	15,600			
1,200	100	22,500			
1,500	100	35,200			

Table IV-2-(20) Resistivity Field Data at K Line, Point 121

AB/2	MN/2	K	I (Amp)	V (mV)	R (Ω m)
3	1	12.6	0.20	1,420	89.5
5	1	37.7	0.20	467	88.0
7	1	75.4	0.20	267	101
10	1	156	0.20	173	135
10	3	47.6	0.20	500	119
15	3	113	0.12	196	185
15	1	352	0.12	67.0	197
20	3	205	0.12	143	244
30	3	467	0.20	162	378
50	3	1,300	0.20	100	650
50	10	377	0.20	316	596
70	10	754	0.20	208	784
70	3	2,560	0.20	66.7	854
100	10	1,560	0.20	108	842
150	10	3,520	0.16	31.7	697
200	10	6,270	0.10	6.83	428
200	50	1,180	0.10	30.8	363
250	50	1,880	0.20	23.3	219
250	10	9,800	0.20	5.33	261
300	50	2,750	0.10	2.67	73.4
400	50	4,950	0.16	2.00	61.9
500	50	7,780	0.30	2.13	55.2
500	100	3,770			
700	100	7,540			
700	50	15,300			
1,000	100	15,600			
1,200	100	22,500			
1,500	100	35,200			

Table IV-2-(21) Resistivity Field Data at M Line, Point 80

AB/2	MN/2	K	I (Amp)	V (mV)	R (Ω m)
3	1	12.6	0.21	2,670	160
5	1	37.7	0.30	1,325	167
7	1	75.4	0.30	950	239
10	1	156	0.30	550	286
10	3	47.6	0.30	1,280	203
15	3	113	0.30	320	121
15	1	352	0.30	260	305
20	3	205	0.30	250	171
30	3	467	0.20	108	252
50	3	1,300	0.30	79.0	342
50	10	377	0.30	127	160
70	10	754	0.30	155	390
70	3	2,560	0.30	48.2	411
100	10	1,560	0.20	52.3	408
150	10	3,520	0.06	7.50	440
200	10	6,270	1.00	65.3	409
200	50	1,180	1.00	290	342
250	50	1,880	0.12	15.8	248
250	10	9,800	0.12	3.58	292
300	50	2,750	0.30	21.7	199
400	50	4,950	0.30	7.30	120
500	50	7,780	0.30	2.03	52.6
500	100	3,770			
700	100	7,540			
700	50	15,300			
1,000	100	15,600			
1,200	100	22,500			
1,500	100	35,200			

Table IV-2-(22) Resistivity Field Data at M Line, Point 85

AB/2	MN/2	K	I (Amp)	V (mV)	R (Ω m)
3	1	12.6	0.20	1,770	112
5	1	37.7	0.20	730	138
7	1	75.4	0.16	310	146
10	1	156	0.16	164	160
10	3	47.6	0.16	400	119
15	3	113	0.16	147	104
15	1	352	0.16	62.0	136
20	3	205	0.30	143	97.7
30	3	467	0.30	70.7	110
50	3	1,300	0.30	25.8	112
50	10	377	0.30	91.3	115
70	10	754	0.12	20.2	127
70	3	2,560	0.10	4.70	120
100	10	1,560	0.16	17.3	169
150	10	3,520	0.20	13.3	234
200	10	6,270	0.20	8.63	271
200	50	1,180	0.20	35.8	211
250	50	1,880	0.20	23.8	224
250	10	9,800	0.20	5.87	288
300	50	2,750	0.20	15.1	208
400	50	4,950	0.50	14.3	142
500	50	7,780	0.30	2.93	76.0
500	100	3,770			
700	100	7,540			
700	50	15,300	0.80	1.61	30.8
1,000	100	15,600			
1,200	100	22,500			
1,500	100	35,200			

Table IV-2-(23) Resistivity Field Data at M Line, Point 90

AB/2	MN/2	K	I (Amp)	V (mV)	R (Ω m)
3	1	12.6	0.20	1,250	78.8
5	1	37.7	0.20	310	58.4
7	1	75.4	0.20	142	53.5
10	1	156	0.20	81.7	63.7
10	3	47.6	0.20	242	57 6
15	3	113	0.20	117	66.1
15	1	352	0.20	42.5	74.8
20	3	205	0.10	33.3	68.3
30	3	467	0.12	22.5	87.6
50	3	1,300	0.16	8.10	65.8
50	10	377	0.16	29.5	69.5
70	10	754	0.10	6.83	51.5
70	3	2,560	0.10	1.96	50.2
100	10	1,560	0.20	4.17	32.5
150	10	3,520	0.20	1.13	19.9
200	10	6,270	0.30	0.757	15.8
200	50	1,180	0.30	6.23	24.5
250	50	1.880	0.30	4.28	26.8
250	10	9,800	0.30	0.543	17.7
300	50	2,750	0.30	3.17	29.1
400	50	4,950	0.30	2.08	34.3
500	50	7,780	0.20	0.89	34.6
500	100	3,770	0.20	2.19	41.3
700	100	7,540	0.12	0.467	29.3
700	50	15,300	0.12	0.22	28.1
1,000	100	15,600	0.30	0.333	17.3
1,200	100	22,500			
1,500	100	35,200			

Table IV-2-(24) Resistivity Field Data at M Line, Point 95

AB/2	MN/2	K	I (Amp)	V (mV)	R (Ω m)
3	1	12.6	0.20	2,870	181
5	1	37.7	0.20	1,180	222
7	1	75.4	0.20	533	201
10	1	156	0.16	133	130
10	3	47.6	0.16	510	152
15	3	113	0.16	138	97.5
15	1	352	0.16	38.0	83.6
20	3	205	0.16	45.8	58.7
30	3	467	0.16	15.5	45.2
50	3	1,300	0.16	5.17	42.0
50	10	377	0.16	17.5	41.2
70	10	754	0.20	10.8	40.7
70	3	2,560	0.20	3.17	40.6
100	10	1,560	0.20	4.17	32.5
150	10	3,520	0.20	1.67	29.4
200	10	6,270	0.30	0.993	20.8
200	50	1,180	0.30	4.93	19.4
250	50	1,880	0.20	1.88	17.7
250	10	9,800	0.20	0.383	18.8
300	50	2,750			
400	50	4,950	0.20	0.65	16.1
500	50	7,780	0.20	0.40	15.6
500	100	3,770	0.20	1.08	20.4
700	100	7,540	0.30	0.61	153
700	50	15,300	0.30	0.22	11.2
1,000	100	15,600	0.20	0.167	13.0
1,200	100	22,500	0.30	0.147	11.0
1,500	100	35,200			
300	10	14,100	0.20	0.267	18.8

Table IV-2-(25) Resistivity Field Data at M Line, Point 100

AB/2	MN/2	K	I (Amp)	V (mV)	R (Ω m)
3	1	12.6	0.10	1,480	186
5	1	37.7	0.10	390	147
7	1	75.4	0.10	142	107
10	1	156	0.20	105	81.9
10	3	47.6	0.20	360	85.7
15	3	113	0.20	156	88.1
15	1	352	0.20	50.7	89.2
20	3	205	0.20	86.7	88.9
30	3	467	0.20	29.7	69.3
50	3	1,300	0.20	9.70	63.1
50	10	377	0.20	34.6	65.2
70	10	754	0.20	13.5	50.9
70	3	2,560	0.20	3.88	49.7
100	10	1,560	0.20	5.23	40.8
150	10	3,520	0.20	2.25	39.6
200	10	6,270	0.06	0.29	30.3
200	50	1,180	0.10	2.82	33.3
250	50	1,880	0.20	3.62	34.0
250	10	9,800	0.20	0.87	42.6
300	50	2,750	0.20	2.49	34.2
400	50	4,950	0.06	0.23	19.0
500	50	7,780	0.30	0.663	17.2
500	100	3,770	0.30	1.48	18.6
700	100	7,540	0.80	2.13	20.1
700	50	15,300	0.80	0.947	18.1
1,000	100	15,600	0.20	0.25	19.5
1,200	100	22,500	0.30	0.223	16.7
1,500	100	35,200	0.80	0.342	15.0

Table IV-2-(26) Resistivity Field Data at M Line, Point 105

AB/2	MN/2	K	I (Amp)	V (mV)	R (Ω m)
3	1	12.6	0.10	447	56.3
5	1	37.7	0.20	418	78.8
7	1	75.4	0.20	217	81.8
10	1	156	0.20	121	94.4
10	3	47.6	0.20	327	77.8
15	3	113	0.20	158	89.3
15	1	352	0.20	59.3	104
20	3	205	0.14	54.7	80.1
30	3	467	0.14	24.2	80.7
50	3	1,300	0.14	6.87	63.8
50	10	377	0.14	23.3	62.7
70	10	754			
70	3	2,560			
100	10	1,560	0.12	3.87	50.3
150	10	3,520	0.08	0.908	40.0
200	10	6,270	0.20	2.50	78.4
200	50	1,180	0.20	7.00	41.3
250	50	1,880	0.30	5.70	35.7
250	10	9,800	0.30	0.983	32.1
300	50	2,750	0.30	4.17	38.2
400	50	4,950	0.20	1.63	40.3
500	50	7,780	0.20	1.13	44.0
500	100	3,770	0.20	3.30	62.2
700	100	7,540	0.08	0.543	51.2
700	50	15,300	0.06	0.153	39.0
1,000	100	15,600	0.30	0.773	40.2
1,200	100	22,500	0.80	1.30	36.6
1,500	100	35,200			
100	3	5,230	0.12	1.21	52.7

Table IV-2-(27) Resistivity Field Data at M Line, Point 110

AB/2	MN/2	K	I (Amp)	V (mV)	R (Ω m)
3	1	12.6	0.20	7,030	443
5	1	37.7	0.20	2,000	377
7	1	75.4	0.20	900	339
10	1	156	0.16	300	293
10	3	47.6	0.16	1,330	396
15	3	113	0.16	367	259
15	1	352	0.16	92.3	203
20	3	205	0.12	85.0	145
30	3	467	0.10	20.3	94.8
50	3	1,300	0.16	10.0	81.3
50	10	377	0.16	42.5	100
70	10	754	0.16	17.1	80.6
70	3	2,560	0.16	4.17	66.7
100	10	1,560			
150	10	3,520	0.10	1.42	50.0
200	10	6,270	0.50	2.50	31.4
200	50	1,180	0.50	16.7	39.4
250	50	1,880	0.30	6.17	38.7
250	10	9,800	0.30	0.975	31.9
300	50	2,750	0.16	2.04	35.1
400	50	4,950	0.08	0.533	33.0
500	50	7,780	0.30	1.00	25.9
500	100	3,770	0.30	1.88	23.6
700	100	7,540	0.30	0.833	20.9
700	50	15,300	0.16	0.25	23.9
1,000	100	15,600	0.50	0.517	16.1
1,200	100	22,500			
1,500	100	35,200			

Table IV-2-(28) Resistivity Field Data at M Line, Point 115

AB/2	MN/2	K	I (Amp)	V (mV)	R (Ω m)
3	1	12.6	0.08	2,900	457
5	1	37.7	0.16	1,770	417
7	1	75.4	0.16	470	221
10	1	156	0.06	40.8	106
10	3	47.6	0.06	245	194
15	3	113	0.08	77.0	109
15	1	352	0.08	17.1	75.2
20	3	205	0.122	58.7	98.6
30	3	467	0.10	17.3	80.8
50	3	1,300	0.162	4.40	35.3
50	10	377	0.162	20.8	48.4
70	10	754	0.077	3.32	32.5
70	3	2,560	0.077	0.742	24.7
100	10	1,560	0.10	1.81	28.2
150	10	3,520	0.16	1.26	27.7
200	10	6,270	0.18	0.853	29.7
200	50	1,180	0.18	5.93	38.9
250	50	1,880	0.20	4.38	41.2
250	10	9,800	0.20	0.65	31.9
300	50	2,750	0.30	4.42	40.5
400	50	4,950	0.30	2.27	37.5
500	50	7,780	0.30	0.923	23.9
500	100	3,770			
700	100	7,540			
700	50	15,300	1.20	1.25	15.9
1,000	100	15,600			
1,200	100	22,500			
1,500	100	35,200			

Table IV-2-(29) Resistivity Field Data at M Line, Point 120

AB/2	MN/2	K	I (Amp)	V (mV)	R (Ω m)
3	1	12.6	0.08	3,330	524
5	1	37.7	0.16	1,880	443
7	1	75.4	0.20	1,030	388
10	1	156	0.20	370	289
10	3	47.6	0.20	1,000	238
15	3	113			
15	1	352			
20	3	205			
30	3	467	0.20	90.7	212
50	3	1,300	0.20	28.7	187
50	10	377	0.20	79.3	149
70	10	754	0.20	33.8	127
70	3	2,560	0.20	12.3	157
100	10	1,560	0.20	15.9	124
150	10	3,520	0.20	5.80	102
200	10	6,270	0.20	2.83	88.7
200	50	1,180	0.20	10.4	61.4
250	50	1,880	0.08	2.43	57.1
250	10	9,800	0.08	0.69	84.5
300	50	2,750	0.08	1.29	44.3
400	50	4,950	0.16	1.65	51.0
500	50	7,780	0.30	2.03	52.6
500	100	3,770			
700	100	7,540			
700	50	15,300			
1,000	100	15,600			
1,200	100	22,500			
1,500	100	35,200			

APPENDICES

I X-RAY DIFFRACTION DATA FOR ALTERED ROCKS

Appendix 1

X-ray Diffraction Data for Altered Rocks

No.	Sample No.	Lithology \ Minerals	Silica minerals			Altered minerals							Sulfates & carbonates			Others				Primary minerals					
			α–Cristobalite	β–Cristobalite	α–Quartz	Allophane (amorphous)	Montmorillonite	Montmorillonite/Kaolinite	Kaolinite	Pyrophyllite	Boemite	Clinoptilolite	Alunite	Alunogen	Calcite	Magnetite	Hematite	Marcasite	Sinhalite	Feldspar	Hornblende	Aenigmatite	Augite	Acmite	Mica
1	E–2	clay (white)			◎				◎																
2	E–3	clay (reddish brown)			△	△	○		△											△					
3	E–4	clay (brownish white)		◎	△				◎																
4	E–5	clay (yellowish grey)			△		◎		◎											•					
5	E–6	clay (white)			◎				◎																
6	E–7	altered rock (brownish grey)			◎		△		△											○					
7	E–9	porous altered rock (pinkish brown)			◎		△													○	•				
8	E–11	clay (white)			◎				◎																
9	E–14	porous altered rock (white)		◎	△				○	?															
10	E–15	silicified rock (white)		◎	△				◎																
11	E–16	argillized rock (white)			△				◎																
12	E–18	altered rock (yellowish brown)		○	◎					?										○					
13	E–20	obsidian (dark green)			○															◎	△				•
14	E–21	clay (yellow)			◎				△											△	△				
15	E–22	porous altered obsidian (dark green)			◎		△		•											○	△				
16	E–23	porous obsidian (pale green)			△	•				?										○	△				
17	E–26	porous obsidian (dark green~dark brown)			○															○	△				
18	E–28	obsidian (greenish grey)			◎															○	○				
19	E–30	obsidian (yellowish grey)			△	•		•				•								○	•				•
20	E–31	altered obsidian (yellowish brown)			•	△														△					
21	E–33	porous altered obsidian			○			△												◎	○			△	
22	E–34	pumice				△			•											△					
23	E–36	obsidian (brown)			○			•												○	△				•
24	E–37	obsidian			△	•														○	○				

X-ray Diffraction Data for Altered Rocks

No.	Sample No.	Lithology \ Minerals	Silica minerals				Altered minerals								Sulfates & carbonates				Others				Primary minerals						
			α–Cristobalite	β–Cristobalite	α–Quartz		Allophane (amorphous)	Montmorillonite	Montmorillonite/Kaolinite	Kaolinite	Pyrophyllite	Boemite	Clinopilolite		Alunite	Alunogen	Calcite		Magnetite	Hematite	Marcasite	Sinhalite	Feldspar	Hornblende	Aenigmatite	Augite	Acmite	Mica	
25	E–38	clay (pale yellowish grey)			•			○															△	◎					
26	E–40	ditto			△			◎															△	△					
27	E–41	clay with brownish stain			△				◎														△	△				•	
28	E–42	clay (reddish brown, partly yellowish grey)			△				○	△													△						
29	E–43	obsidian (pale greenish grey)			○																		○				○		
30	E–48	porous obsidian (dark grey)			△		•												△				○	△					
31	E–50	porous silicified rock (reddish brown)	△		◎					○										•			△						
32	E–52	porous obsidian (dark greenish grey)	•		△		•																○	△					
33	E–54	porous obsidian (pale yellow)	○		○				△													?	◎	○					
34	E–55	porous obsidian (grey)			○																		◎	◎					
35	E–56	obsidian (black)			△		•																△	△					
36	E–57	clay (yellowish brown)			△			◎															○	○					
37	E–60	obsidian (dark green)			◎					•													○	○					
38	E–61	porous altered rock (brownish grey)			△		○		•														△	•					
39	E–63	clay (pale green~grey)			◎			○		◎										•									
40	E–66	porous clay (grey)			◎			△															○	○					
41	E–67	clay (reddish brown)			○					○										△			○						
42	E–68	argillized pumice (yellowish green)			◎				△	•													○	○					
43	E–69	argillized pumice (yellowish grey)			○				○	○													○	○					
44	E–71	weakly argillized pumice (reddish brown)			△		△																•						
45	E–73	argillized pumice (dark reddish brown)					•		○	•										•									
46	E–74	porous altered obsidian (dark yellowish grey)			△			◎															◎	△					
47	E–75	porous obsidian (dark grey)			◎					△													◎	○					
48	E–76	obsidian (reddish brown)			◎															△			◎						

X-ray Diffraction Data for Altered Rocks

No.	Sample No.	Lithology \ Minerals	Silica minerals				Altered minerals								Sulfates & carbonate				Others				Primary minerals						
			α–Cristobalite	β–Cristobalite	α–Quartz		Allophane (amorphous)	Montmorillonite	Montmorillonite/Kaolinite	Kaolinite	Pyrophyllite	Boemite	Clinoptilolite		Alunite	Alunogen	Calcite		Magnetite	Hematite	Marcasite	Sinhalite	Feldspar	Hornblende	Aenigmatite	Augite	Acmite	Mica	
49	E–77	argillized obsidian (dark reddish brown)			◎					△										△			○					•	
50	E–80–2	obsidian (greenish grey)			◎																		○				△		
51	E–81	porous basalt (dark brown)			•			◎									○			△						○			
52	E–83	ditto						○												△			◎			△			
53	E–85	obsidian (bluish grey)			◎																		◎	○			△		
54	E–89	phonolite (yellowish grey~brown)			◎					•													○	△				•	
55	E–91	argillized obsidian (brown)			◎															•			◎						
56	E–93	porous basalt																					◎			○			
57	E–95	altered rock (reddish brown)			○				△											△			◎	△					
58	E–97	argillized obsidian (yellowish brown)						○															◎						
59	E–98	altered obsidian (pale yellow~brown)			◎																		○						
60	E–99	porous altered obsidian (reddish brown)			○															•			◎	•					
61	E–100	porous obsidian (dark green)			○				•											•			◎	△	△				
62	E–101	argillized obsidian (reddish brown)			△				△	△										△			○	△					
63	E–104	argillized obsidian (brown)		△	◎		△										△												
64	E–105	weakly argillized obsidian (yellowish~reddish brown)							◎				○																
65	E–106	strongly argillized obsidian (brown)							◎	•																			
66	E–108	porous basalt						○															◎			○			
67	E–109	argillized obsidian (bluish white)			○					◎																			
68	E–110	clay (grey)			○					◎		○																	
69	E–111	clay (white)								◎																			
70	E–112	clay (pinkish white)			○					◎																			
71	E–113	clay (white)			△					◎																			
72	E–115	porous argillized rock (white)			△					◎	?																		

X-ray Diffraction Data for Altered Rocks

No.	Sample No.	Lithology \ Minerals	Silica minerals				Altered minerals								Sulfates & carbonates				Others				Primary minerals						
			α–Cristobalite	β–Cristobalite	α–Quartz		Allophane (amorphous)	Montmorillonite	Montmorillonite/Kaolinite	Kaolinite	Pyrophyllite	Boemite	Clinopilolite		Alunite	Alunogen	Calcite		Magnetite	Hematite	Marcasite	Sinhalite		Feldspar	Hornblende	Aenigmatite	Augite	Acmite	Mica
73	E–116	porous argillized rock (white)			◎					◎					◎														
74	E–117	ditto			△		△			◎																			
75	E–118	weakly altered obsidian (black)					•			•																			
76	E–119	strongly altered obsidian (reddish brown)			•					△										•				•					
77	E–121	porous altered obsidian (pale yellowish grey)	◎							•														○	○				
78	E–122	porous altered obsidian (dark brown)					•			•														•					
79	E–123	porous obsidian (dyke)			◎				△											△				◎	•	•			
80	E–124	banded obsidian (dyke)							○															◎					
81	E–125	weakly altered obsidian (dyke)	○		○			○																◎	△				
82	E–126	strongly altered obsidian (yellowish brown)	◎		○			○																○					
83	E–128	porous obsidian (pale green)		△	•		•			•										△				△					
84	E–130	spotted, argillized pumice (yellowish grey~reddish brown)			△			◎		•														△					
85	E–131	banded, altered obsidian (pale green)	◎		•																			△	△				
86	E–132	argillized obsidian (reddish brown)			△				•	○										△				△					
87	E–134	porous altered obsidian (greenish grey)			◎																			○	△			△	
88	E–135	porous altered obsidian (grey)	△		△																			○	△				
89	E–136	porous basalt (reddish brown)							•											△				◎			◎		
90	E–137	porous argillized rock (white)	○		◎					◎																			
91	E–139	ditto			◎					◎																			
92	E–140	porous silicified rock (greenish grey)	△	◎	◎					○																			
93	E–143	clay (pale grey)			○					○					◎														
94	E–146	altered silicified rock (white)		◎	△					○																			
95	E–147	clay (pinkish white)		◎	○					◎																			
96	E–148	altered rock (white)			○					○						△													

X-ray Diffraction Data for Altered Rocks

No.	Sample No.	Lithology \ Minerals	Silica minerals				Altered minerals								Sulfates & carbonates				Others				Primary minerals						
			α–Cristobalite	β–Cristobalite	α–Quartz		Allophane (amorphous)	Montmorillonite	Montmorillonite/Kaolinite	Kaolinite	Pyrophyllite	Boemite	Clinopilolite		Alunite	Alunogen	Calcite		Magnetite	Hematite	Marcasite	Sinhalite	Feldspar	Hornblende	Aenigmatite	Augite	Acmite	Mica	
97	E–149	altered silicified rock (white)		◎	△					○																			
98	E–150	porous argillized rock (white)		◎	△					○																			
99	E–152	porous silicified rock (white)	◎	△	○					◎																			
100	E–153	clay (white)								◎																			
101	E–33				○					△													◎	○			△		
102	E–42				△					○	△												△						
103	E–55				○																		◎	◎					
104	E–73						•			○	•								•										
105	E–98				◎																		○						
106	E–106									◎	•																		
107	E–112				○						◎																		
108	E–128			△	•		•				•									△			△						
109	E–148				○						○				△														
110	E–152		◎	△	○						◎																		

Symbols : ◎ abundunt, ○ common, △ a little, • rare, ? uncertain

LIST OF CONTENTS

Fig.Ⅱ-2 Geological Map of the Eburru Prospect

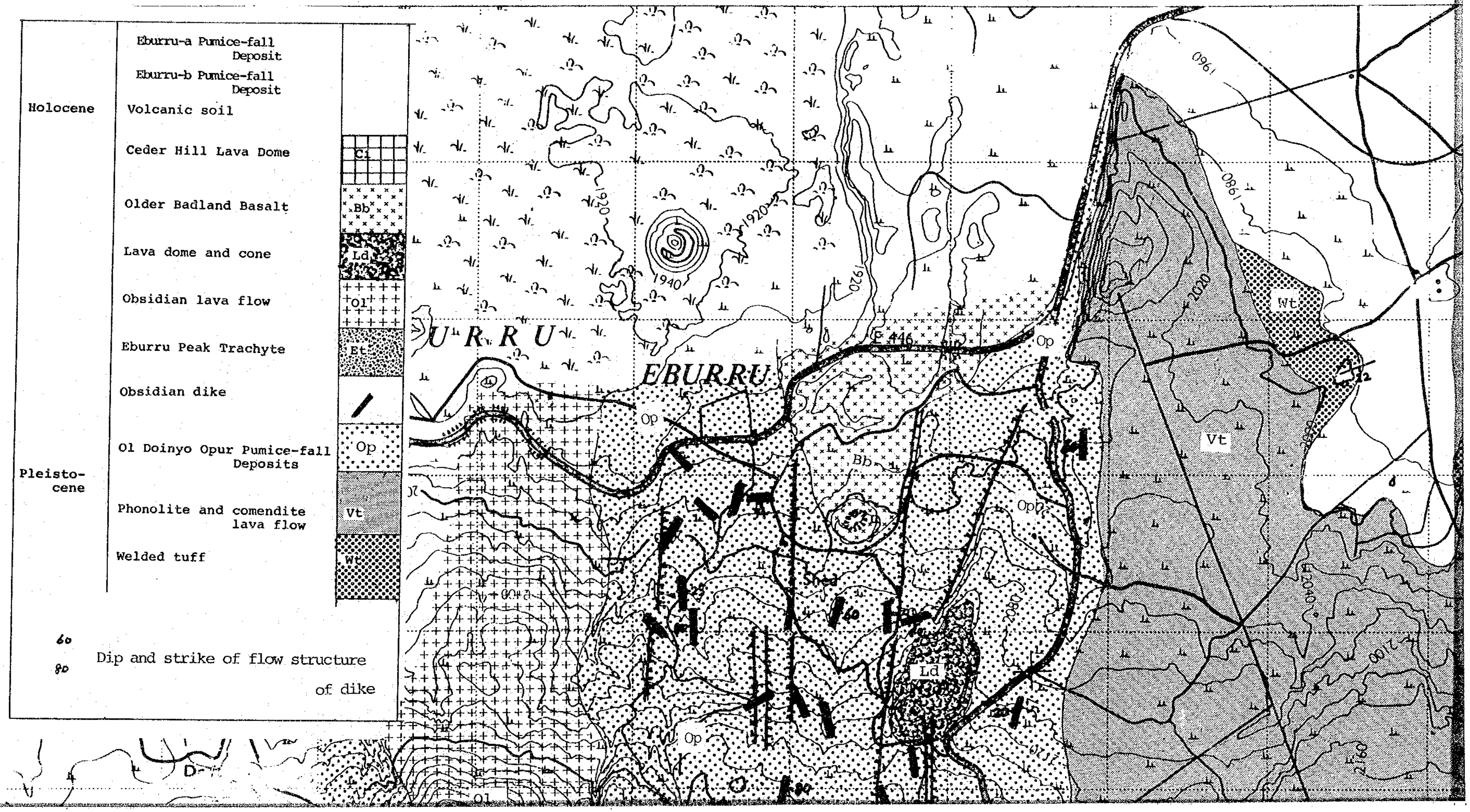

Fig. II-2 Geological Map of the Eburru Prospect